and unlike MAT*a*, the MATα strains posses a 55 kb gene locus responsible for virulence.[24] Although MAT*a* strains have been reported in Tanzania,[22] it was not detected in our study.

All the isolates were susceptible to AMP ($MIC_{90}$ 0.5 μg $ml^{-1}$) in accord with other reports that the MIC to AMP has remained unchanged over time with no evidence of resistance.[12] Although the $MIC_{90}$ was lower than that reported for Malawi (0.5 μg $ml^{-1}$ vs. 2 μg $ml^{-1}$), it further complement reports of isolated strains from African with elevated MIC to AMP[25,26] and calls for continued surveillance.

Resistance to 5FC was unusually high (21.2%) with majority (77.6%) of the isolates having MIC between 8 and 32 μg $ml^{-1}$ in contrast with previous reports of high susceptibility and no instances in which increased MIC to 5FC has been reported.[12] Despites, reports that antifungal susceptibility has improved worldwide, pockets of resistance cannot be ruled out as an exhaustive surveillance has not been conducted in areas where resistance has previously been reported. Moreover, there are emerging reports that the epidemiology and drug susceptibility of *C. neoformans* strains from some African countries are different which are possible pockets of resistance.[11,27,28] Although the frequency of 5FC and azole resistance was unusually high, due to lack of proper follow up and ethical reasons we could not link up susceptibility and clinical data to ascertain whether patients infected with these resistant strains had poor prognosis. We hope this will address in our newly proposed study which will also collect more of such isolates to be tested using CLSI broth microdilution technique.

Fluconazole resistance was detected at a frequency of 11.2% while the $MIC_{90}$ of ITC and MCZ were 0.5 and 2 μg $ml^{-1}$ respectively. In Spain, reduced susceptibility to FLC and 5FC has been reported with resistance of 5.3% and 15.8% to AMP and ITC while decreased susceptibility to azoles associated with fungal burden and immunosuppression has been reported.[29,30] Similar pattern have been reported in Cambodia and other developing countries and is associated with FLC maintenance therapy in AIDS.[11,31,32] While an overall shift towards susceptibility to FLC and 5FC attributed to decrease incidence of cryptococcosis and effective antiretroviral programmes in the USA and Europe may be true, this is unlikely in developing countries particularly sub-Saharan Africa where the prevalence of HIV/AIDS and crytococcal meningitis continue to increase. Susceptibility to FLC has been shown to improve in AIDS patients on highly active antiretroviral therapy (HAART),[33] while this may be the case in USA and Europe, unfortunately <1% of AIDS patients in sub-Saharan African are on HAART.

The reasons for the low susceptibility to FLC were not apparently clear in our study but it is notable that the isolates were recovered from AIDS patients from an urban referral hospital. Being a referral hospital majority of the patients were likely to have been previously exposed to FLC or were relapse cases this; however, could not be confirmed in our study. Reduced susceptibility to FLC has been noted in AIDS and in patients with recurrent meningitis. Furthermore, it has been demonstrated that serial isolates of *C. neoformans* from AIDS patients have altered virulence-related factors and drug susceptibilities.[14,15] However, we further speculate that poor prescription practices and under dosages may be confounding factors. Although earlier studies show improved antifungal susceptibility it does not indicate whether the strains included those from Kenya or sub-Saharan African with the highest burden of HIV/AIDS. Improved susceptibility in developed countries is possible due to accessibility and affordability of other effective triazoles, declining rates of HIV/AIDS and cryptococcoses, effective HAART programmes and good prescription practices which is not the case in sub-Saharan Africa. The hidden dangers of FLC maintenance therapy in HIV/AIDS in poor resource countries in sub-Saharan Africa cannot still be under estimated.

Clinical response to fluconzole is likely only when the MIC is <16 μg $ml^{-1}$[34] and FLC resistance rate of 11.2% for a developing country like Kenya is intriguing and may be a reflection of poor prognosis currently witnessed in patients with meningoencephalitis in Kenya. As FLC becomes increasingly used due to the need for life-long maintenance therapy in HIV/AIDS patients, we recommend measures to control irrational use of antifungal drugs and establishment of constant antifungal drug resistant surveillance in sub-Saharan Africa where emerging resistance is more likely.

## Acknowledgments

This investigation on Research and Control of Opportunistic Infections was supported by grants from the Japanese International Cooperation Agency (JICA) and Kenya Medical Research Institute (KEMRI). Authentic strains were kindly provided by Dr R. Kano and Professor A. Hasegawa of Nihon University School of Veterinary Medicine.

This work is published with the permission of the Director KEMRI.



 

## Reference


1 Mitchell TG, Perfect JR. Cryptococcosis in the era of AIDS-100 years after the discovery of *Cryptococcus neoformans*. *Clin Microbiol Rev* 1995; **8**: 515–48.

2 Steenbergen JN, Casadevall A. Prevalence of *Cryptococcus neoformans* var. *neoformans* (serotype D) and *Cryptococcus neoformans* var. *grubii* (serotype A) isolates in New York City. *J Clin Microbiol* 2000; **32**: 1974–1976.

3 Goldman DL, Khine H, Abadi J *et al.* Serological evidence of *Cryptococcus neoformans* infection in early childhood. *Pediatrics* 2001; **107**: e66.

4 Bogaerts J, Rouvroy D, Taelman H *et al.* AIDS-associated cryptococcal meningitis in Rwanda (1983–1992): epidemiologic and diagnostic features. *J Infect* 1999; **39**: 32–7.

5 Heyderman RS, Gangaidzo IT, Hakim JG *et al.* Cryptococcal meningitis in human immunodeficiency virus-infected patients in Harare, Zimbabwe. *Clin Infect Dis* 1998; **26**: 284–9.

6 Franzot SP, Salkin IF, Casadevall A. *Cryptococcus neoformans* var. *grubii*: separate varietal status for *Cryptococcus neoformans* serotype A isolates. *J Clin Microbiol* 1999; **37**: 838–40.

7 Kwon-Chung KJ. A new species of *Filobasidiella*, the sexual state of *Cryptococcus neoformans* B and C serotypes. *Mycologia* 1976; **68**: 942–5.

8 Kwong-Chung KJ, Bennett JE. High prevalence of *Cryptococcus neoformans* var. *gattii* in tropical and subtropical regions. *Zentralbl Bakteriol Mikrobiol Hyg A* 1984; **257**: 213–8.

9 Nielsen K, Cox GM, Wang P *et al.* Sexual cycle of *Cryptococcus neoformans* var. *grubii* and virulence of congenic *a* and α isolates. *Infect Immun* 2003; **71**: 4831–41.

10 Boekhout T, Theelen B, Diaz M *et al.* Hybrid genotypes in the pathogenic yeast *Cryptococcus neoformans*. *Syst Evol* 2001; **147**: 891–907.

11 Chandenier J, Adou-Bryn KD, Douchet C *et al.* In vitro activity of amphotericin B, fluconazole and voriconazole against 162 *Cryptococcus neoformans* isolates from Africa and Cambodia. *Eur J Clin Microbiol Infect Dis* 2004; **23**: 506–8.

12 Pfaller MA, Messer SA, Boyken L *et al.* Global trends in the antifungal susceptibility of *Cryptococcus neoformans* (1990 to 2004). *J Clin Microbiol* 2005; **43**: 2163–7.

13 Pfaller MA, Zhang J, Messer SA *et al. In vitro* activities of vericonazole, fluconazole and itraconazole against 566 clinical isolates of *Cryptococcus neoformans* from United States and Africa. *Antimicrob Agents Chemother* 1999; **43**: 169–71.

14 Paugam A, Blanche DP, Gangnenux JP, Tourte-Schaefer C, Sicard D. Increased fluconazole resistance of *Cryptococcus neoformans* isolated from patients with AIDS and recurrent meningitis. *Clin Infect Dis* 1994; **19**: 975–6.

15 Berg J, Clancy CJ, Nguyen MH. The hidden dangers of primary fluconazole prophylaxis for patients with AIDS. *Clin Infect Dis* 1998; **26**: 186–7.

16 Makimura K, Suzuki T, Tamura T *et al.* Comparative evaluation of standard dilution method and commercial kit for frozen plate antifungal susceptibility testing of yeasts using 200 clinical isolates. *Microbiol Immunol* 2004; **48**: 747–53.

17 National Committee for Clinical Laboratory Standards. *Reference Method for Broth Dilution Antifungal Susceptibility Testing of Yeasts; Approved Standard*, 2nd edn, Document M27-A2. Wayne, PA: National Committee for Clinical Laboratory Standards, 2002.

18 Makimura K, Oguri T, Mikami Y *et al.* Multicenter evaluation of commercial frozen plates for microdilution broth antifungal susceptibility testing of yeasts and comparison of MIC limits recommended in NCCLS M27-A2. *Microbiol Immunol* 2005; **49**: 97–106.

19 Garcia-Hermaso D, Janbon G, Drome F. Epidemiological evidence for dormant *Cryptococcus neoformans* infection. *J Clin Microbiol* 1999; **37**: 3204–9.

20 Ellis DH, Pfeiffer TJ. Natural habitat of *Cryptococcus neoformans* var. *gattii*. *J Clin Microbiol* 1990; **28**: 1642–4.

21 Litvintseva AP, Marra RE, Nielsen K *et al.* Evidence of sexual recombination among *Cryptococcus neoformans* serotype A isolates in sub-Saharan Africa. *Eukaryot Cell* 2003; **2**: 1162–8.

22 Lengeler KB, Wang P, Cox GM, Perfect JR, Heitman J. Identification of the MATa mating-type locus of *Cryptococcus neoformans* reveals a serotype A MATα strain thought to have been extinct. *Proc Natl Acad Sci USA* 2000; **97**: 14455–60.

23 Nielsen K, Cox GM, Wang P *et al.* Sexual cycle of *Cryptococcus neoformans* var. *grubii* and virulence of congenic α and alpha isolates. *Infect Immun* 2003; **71**: 4831–41.

24 Chang YC, Winkers BL, Miller GF, Penoger LA, Kwon-Chung KJ. *Cryptococcus neoformans* STE12α regulates virulence but is not essential for mating. *J Exp Med* 2000; **191**: 871–82.

25 Neil F, Katherine G, Watera C *et al. Cryptococcus* infection in a cohort of HIV-1-infected Ugandan adults. *AIDS* 2000; **16**: 1031–8.

26 Powderly WG, Keath EJ, Sokol-Anderson M *et al.* Amphotericin B-resistant *Cryptococcus neoformans* in a patient with AIDS. *Infect Dis Clin Pract* 1992; **1**: 314–6.

27 Archibald LK, Tuohy MJ, Wilson DA *et al.* Antifungal susceptibilities of *Cryptococcus neoformans*. *Emerg Infect Dis* 2004; **10**: 143–5.

28 Pfaller M, Zhang J, Messer S *et al.* Molecular epidemiology and antifungal susceptibility of *Cryptococcus neoformans* isolates from Uganda AIDS patients. *Diagn Microbiol Infect Dis* 1998; **32**: 191–9.

29 Cuenca-Estrella M, Diaz-Guerra TM, Mellado E, Rodriguez-Tudela JL. Flucytosin primary resistance in *Candida* species and *Cryptococcus neoformans*. *Eur J Clin Microbiol Infect Dis* 2001; **20**: 276–9.

30 Perkins A, Gomez-Lopez A, Mellodo E, Rodriguez-Tudela JL, Guenca-Estrella M. Rates of antifungal resistance


 

among Spanish clinical isolates of *Cryptococcus neoformans* var. *neoformans*. *J Antimicrob Chemother* 2005; **56**: 1144–7.

31 Sar B, Monchy D, Vann M, Keo C, Sarthou JL, Buisson Y. Increasing in vitro resistance to fluconazole in *Cryptococcus neoformans* Cambodian isolates: April 2000 to March 2002. *J Antimicrob Chemother* 2004; **54**: 563–5.

32 Datta K, Jain N, Sethi S, Rattan A, Casadevall A, Banerjee U. Fluconazole and itraconazole susceptibilities of clinical isolates of *Cryptococcus neoformans* at a tertiary care centre in India; a need for care. *J Antimicrob Chemother* 2003; **52**: 683–6.

33 Martins MD, Lozano-Chiu M, Rex JJ. Declining rates of oropharyngeal candidiasis and carriage of *Candida albicans* associated with trends toward reduced rates of carriage of fluconazole-resistant *C. albicans*. *Clin Infect Dis* 1998; **27**: 1291–12.

34 Aller AI, Martin-Mazuelos E, Lozano F *et al.* Correlation of fluconazole MICs with clinical outcome in cryptococcal infection. *Antimicrob Agents Chemother* 2000; **44**: 1544–8.



 

INTERNAL MEDICINE

CASE REPORT

# An Outbreak of Histoplasmosis among Healthy Young Japanese Women after Traveling to Southeast Asia

Hideaki Ohno[1], Yoshiko Ogata[2], Hajime Suguro[3], Soichiro Yokota[4], Akira Watanabe[5], Katsuhiko Kamei[5], Satoshi Yamagoe[1], Akiko Ishida-Okawara[1], Yukihiro Kaneko[1], Atsuko Horino[6], Kunikazu Yamane[6], Takahiro Tsuji[7], Noriyo Nagata[7], Hideki Hasegawa[7], Yoshichika Arakawa[6], Tetsutaro Sata[7] and Yoshitsugu Miyazaki[1]

## Abstract

Histoplasmosis, caused by *Histoplasma capsulatum*, is an endemic mycosis in many countries of the world except for Japan. Outbreaks of histoplasmosis among Japanese people are very rare and are mainly imported by travelers. We report an outbreak of histoplasmosis among healthy Japanese people who traveled to a resort area in Southeast Asia. Three young Japanese women traveled to Langkawi island, Malaysia and stayed on the island for five days without visiting caves, a known reservoir of *H. capsulatum*. All three individuals developed flu-like symptoms with multiple nodule shadows on chest X rays or chest CT scans at around ten days after their return to Japan. Serum samples obtained from the three subjects were positive for anti-*Histoplasma* antibody and specific PCR for *H. capsulatum* on lung biopsy specimens and the serum from one patient was positive. The clinical course of all three patients improved without the use of anti-fungal agents and no recurrence has been confirmed. Clinical attendants should consider histoplasmosis when they see patients with flu-like symptoms with abnormal chest X-rays after visiting *H. capsulatum* endemic areas, especially Southeast Asia.

**Key words:** histoplasmosis, outbreak, serological test, PCR

**(Inter Med 49: ☆☆☆-☆☆☆, 2010)**
**(DOI: 10.2169/internalmedicine.49.2759)**

## Introduction

Histoplasmosis is one of the endemic mycoses in North America (Ohio and Mississippi river valleys), Central and South America, Africa, and Asia (1). In Japan, histoplasmosis is considered an imported mycosis because most patients had recently traveled to endemic areas (including cave exploration) and very few had been suspected of domestic infection (2). Although several outbreaks of histoplasmosis have been reported all over the world, most infections have been reported in North and South America (3-7) and few reports describing outbreaks of histoplasmosis among Japanese people (7, 8). Here, we report an outbreak of histoplasmosis in three Japanese women who had visited a resort area in Southeast Asia for which serum and *Histoplasma*-specific PCR tests of lung tissue and blood samples facilitated making a confirmatory diagnosis.

## Case Report

A 27-year-old Japanese woman traveled to Langkawi Island, Malaysia, with two other Japanese friends in November 2007. During her stay, she spent most of her time in a

[1]Department of Chemotherapy and Mycoses, National Institute of Infectious Diseases, Tokyo, [2]National Hospital Organization, Yamaguchi-Ube Medical Center, ☆☆, [3]Department of Respiratory Medicine, Yokohama Social Insurance Chuo Hospital, ☆☆, [4]Division of Respiratory Disease, National Hospital Organization Toneyama National Hospital, ☆☆, [5]Division of Fungal Infection, Medical Mycology Research Center, Chiba University, ☆☆, [6]Department of Bacteriology II, National Institute of Infectious Diseases, ☆☆ and [7]Department of Pathology, National Institute of Infectious Diseases, ☆☆
Received for publication August 11, 2009; Accepted for publication October 29, 2009
Correspondence to Dr. Yoshitsugu Miyazaki, ym46@nih.go.jp

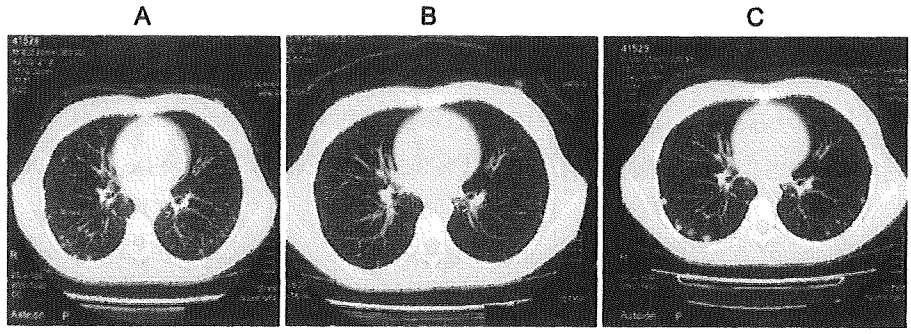


**Figure 1. Time course of chest CT scan images of the patient. A) Multiple small nodules were confirmed in both lung fields during the first visit to the hospital (December 2007). B) The number of nodular shadows decreased and had almost disappeared without specific treatment (January 2008). C) Multiple small nodules were evident in both lungs concurrent with the emergence of back pain (February 2008).**

five-star class resort hotel surrounded by sea and jungle. The woman took all meals and foods in the hotel, did not walk in the jungle and never visited caves. After a five-day stay on the island, she returned to Japan. Ten days after her return, she felt general fatigue with flu-like symptoms (fever of 38℃, headache, and muscle pain) and saw a local doctor. A conventional influenza antigen detection test was performed but was confirmed negative. Symptoms were treated as for the common cold for a duration of 4 days due to a moderate fever. Thereafter, all symptoms subsided.

Twenty days later, the individual developed back pain with dyspnea, and visited a nearby hospital the following day. The woman's condition was almost fully recovered and no significant findings on physical examination were confirmed. Several examinations were performed, and a chest CT scan revealed multiple nodules in bilateral lungs (Fig. 1A). Blood tests, biochemical examination, and serum examination results were as follows: white blood cell count 7,370 cells/μL (47% neutrophils, 31% lymphocytes, 5% monocytes, 5% eosinophils); hemoglobin 13.4 g/dL; C-reactive protein 0.48 mg/dL; all liver function and renal function parameters were within the normal range; urine occult blood (+/-); and WBC (+). Microbiological tests including bacterial and mycological culture of sputum showed the presence of only indigenous bacteria and tests for (1→3)-beta-D-glucan, *Aspergillus* galactomannan antigen, *Candida* mannan, and *Cryptococcal* antigen were all negative. At this time, although some infectious diseases including fungal infections were suspected, no specific treatments were given due to the good condition of the patient, and the clinical course was observed. During the course observation period, no remarkable change in condition was observed and a follow-up chest CT scan revealed improvement of the shadows (Fig. 1B). Approximately two weeks later, the individual felt the return of mild back pain, however, chest X-rays did not show any significant changes. Back pain disappeared within several days and another follow-up chest CT scan was performed again three weeks after the onset of the recent back pain. CT images revealed the return of multiple nodules in bilateral lungs were (Fig. 1C) and, therefore, a lung biopsy under video-assisted thoracoscopy (VATS) was proposed to make a definite diagnosis.

VATS was performed in April 2008 during which a lung biopsy specimen and serum samples were obtained and immediately transferred to National Institute of Infectious Diseases (NIID) in Tokyo, where microbiological and histopathological examinations were performed. Broad bacterial, mycobacterial and mycological examinations of the lung specimen for aerobic and anaerobic bacteria, *Mycobacterium* spp and common fungi were carried out and showed no microorganism growth. Likewise, PCR for *Burkholderia* spp. and *M. tuberculosis* were also negative. Histopathological examination of the lung tissue revealed multiple small, white nodules (Fig. 2A). In addition, granulomas with caseous necrosis-like tubercles were observed by microscopic examination, and the small size (2-4 μm) and round morphology were confirmed by gomori methenamine silver (GMS) (Fig. 2B) and fluorescent (Fungiflora Y) staining.

Aliquots of two serum samples collected from the patient in January and February 2008 were subjected to serological tests to identify fungal diseases. Both patient samples were positive for anti-*Histoplasma* antibody by ELISA (Histoplasma DxSelect™, Focus Diagnostics, Cypress, CA, USA) and, therefore, histoplasmosis was suspected for the patient.

Prior to PCR for the diagnosis of *H. capsulatum*, we investigated the specificity of the PCR against other known fungal and bacterial pathogens. As shown in Fig. 3, this assay is specific for *H. capsulatum*. For the PCR analysis of patient samples, DNA extraction from a portion of the lung specimen was performed using the DNeasy Blood & Tissue Kits (Qiagen, Germany) according to the manufacturer's instructions. Concurrently, another aliquot of serum was mixed with an equal volume of lysis buffer (9), followed by proteinase K and Westase (Takara, Ohtsu, Japan) treatment

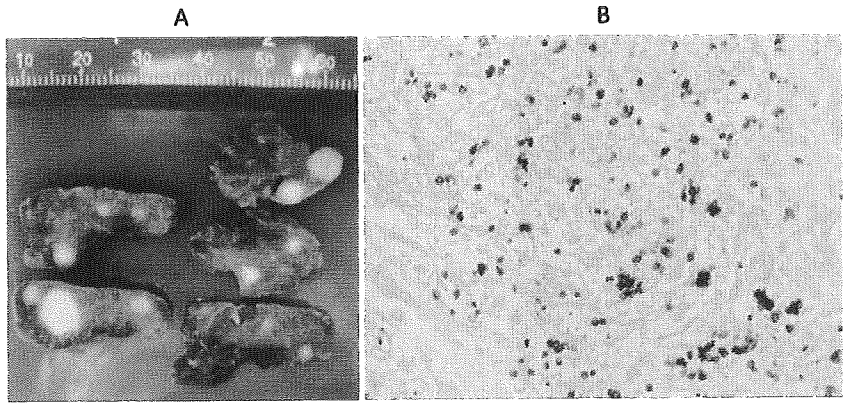


**Figure 2. Histopathological examinations of a lung biopsy specimen. Multiple small, white nodules were observed in lung tissues (A), and GMS staining showed multiple small, rounded morphological yeast-like features (B).**

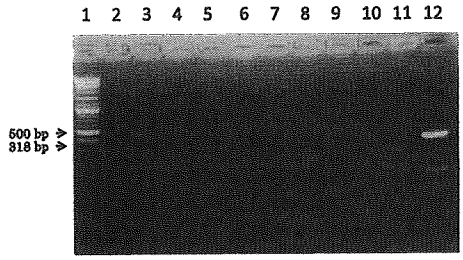


**Figure 3. Agarose gel showing the specificity of the PCR assay (single round PCR: expected amplicon size is 318 bp). DNA was extracted from several fungal species to test the specificity of the PCR. Lane 1, molecular size marker (100 bp ladder); 2, *Aspergillus fumigatus;* 3, *A. niger;* 4, *A. flavus;* 5, *Candida albicans;* 6, *C. glabrata;* 7, *C. parapsilosis;* 8, *Cryptococcus neoformans;* 9, *Trichosporon asahii;* 10, *Penicillium* spp.; 11, *Nocardia brasiliensis* and; 12, *Histoplasma capsulatum.***

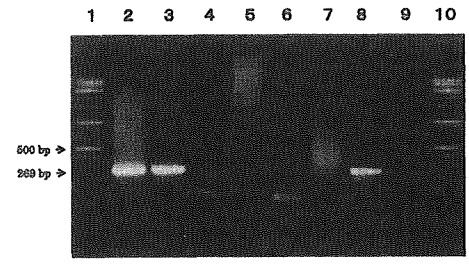


**Figure 4. Agarose gel of products from nested PCR targeting the *Histoplasma capsulatum* M antigen gene in patient samples. Lanes 1 and 10, molecular size marker (100 bp ladder); 2, specimen of lung biopsy DNA; 3, serum sample DNA of the patient; 4, serum sample DNA of another patient (29 years of age, anti-*Histoplasma* antibody positive); 5, serum sample DNA of an unrelated non-infectious disease case (anti-*Histoplasma* antibody negative); 6, serum sample DNA of another patient (28 years of age, anti-*Histoplasma* antibody positive); 7, serum sample DNA of healthy volunteer (anti-*Histoplasma* antibody negative); 8, positive control; 9, negative control.**

and used for PCR. Finally, 5 μL of each sample was used for subsequent PCR. Nested PCR was carried out using our modified sets of primers which amplify a segment of M antigen gene of *H. capsulatum*, as previously reported by de Matos Guedes et al (10). After the second round PCR, 10 μL of each reaction was subjected to agarose gel electrophoresis stained with ethidium bromide. PCR amplicons were confirmed for both the lung specimen and serum samples for the patient (Fig. 4). Furthermore, direct sequencing of positive PCR amplicons was performed for both DNA strands and revealed 99.3% identity with the *H. capsulatum* M antigen gene sequence using the BLAST algorithm. Finally, a confirmed diagnosis of acute pulmonary histoplasmosis was made for the patient.

Similarly, two other women (28 and 29 years old) that had traveled with the first patient to Langkawi Island also developed fever, muscle pain, general fatigue or mild diarrhea at around ten days after their return. These two women were admitted to different hospitals in December 2008 where chest X-rays and CT scans revealed that they both had multiple small nodules on bilateral lungs (Fig. 5). Clinical examinations for diagnosis, including bronchofiberscopic examination, were carried out for each patient but a confirmed diagnosis could not be made. However, one patient showed granuloma formation in the biopsy specimen collected by transbronchial lung biopsy. Several sequential serum samples were collected from both women and frozen for later examination. In May 2008, the serum samples were analyzed at NIID for the presence of anti-*Histoplasma* antibody. The findings confirmed that both patients were positive for antibody to *Histoplasma* as determined by ELISA

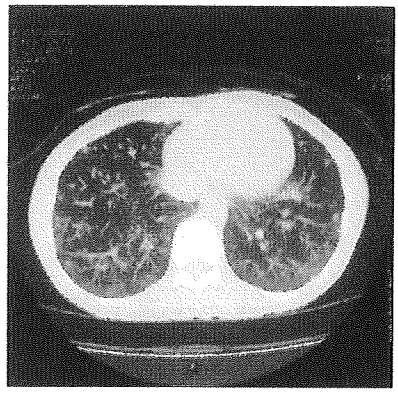

**Figure 5. A chest CT scan image of a 29-year-old woman who also developed flu-like symptoms after returning to Japan (December 2007). The image also revealed multiple small nodules in both lung fields.**

and the diagnosis of suspected histoplasmosis was made. However, the BALF specimen from one patient showed a negative fungal culture and negative *Histoplasma*-specific PCR result, thus a definitive diagnosis could not be obtained.

For all three cases, the individuals were carefully observed during their clinical course and their symptoms and signs gradually disappeared without the need for chemotherapy.

## Discussion

In Japan, the number of histoplasmosis patients has increased dramatically since the mid-1980s, with a total of 63 cases reported as of March 2009 (11). This number is predicted to increase over the next decade as travel abroad is becoming increasingly popular with Japanese people. In this report, all three women had visited Langkawi Island together and all developed flu-like symptoms at approximately the same time after their return to Japan. As all three women reside in different regions of Japan separated from each other by more than two hundred kilometers, it is likely that these women were infected by *H. capsulatum* during their stay on Langkawi Island. The source or reservoir of *H. capsulatum* in the island is unknown but none of the patients visited high-risk areas such as caves. Usually, immunocompetent hosts with *H. capsulatum* infection are asymptomatic or develop mild symptoms (1); however, all three of the young women described in this study showed flu-like symptoms with multiple nodular shadows in the lungs. We speculate that these women had inhaled a high burden of *H. capsulatum* and/or were possibly exposed to a highly virulent strain of *H. capsulatum*. Further studies including environmental surveys are expected.

Clinical laboratory methods for *Histoplasma* detection are likely to become important due to the projected increase in the number of patients. Typically, histoplasmosis is diagnosed using fungal culture, antigen detection methods, serological tests, or histopathological examination (12). Culture of *H. capsulatum* in the clinical laboratory is difficult as it is classified as a biosafety level-3 (BSL-3) pathogen, and it takes approximately four weeks for *H. capsulatum* to grow *in vitro*. Additionally, the sensitivity of fungal culture is reported as relatively low (12), especially in the case of acute pulmonary histoplasmosis. In this report, *H. capsulatum* isolates could not be recovered for all three cases but specimen storage conditions may have influenced these results.

Serological testing for histoplasmosis cases is considered a highly sensitive assay but is reduced for acute histoplasmosis or disseminated disease. In contrast, the antigen detection assay for *H. capsulatum* has been reported as useful in clinical settings with a 75% sensitivity of detection for acute pulmonary histoplasmosis cases but it can cross-react with other pathogens such as coccidiomycosis, paracoccidiomycosis, and blastomycosis (12). In this report, although we could not confirm infection by *H. capsulatum* using the antigen assay, all three cases were positive for antibody and these results helped make the diagnoses. Generally, antibody assays can be used to detect previously infected individuals with no signs of active disease. However, histoplasmosis is not endemic in Japan and the majority of the Japanese population has never been to regions with endemic *H. capsulatum* and, therefore, would be negative for antibody to the organism. To determine if this is indeed the case in Japan, a comprehensive epidemiological study is needed.

Diagnostic methods, such as PCR, are powerful tools for the diagnosis of some infectious diseases but the usefulness of genetic detection methods against fungal diseases is still controversial (12). In this report, we used PCR for the diagnosis of histoplasmosis and confirmed that this assay is specific for *H. capsulatum* (Fig. 3) and could detect at least 1 fg of genomic DNA (data not shown). Therefore, this technique was considered to be another useful method for the diagnosis of histoplasmosis. The PCR assay described here could detect one out of three cases using a lung specimen and serum samples and this may reflect the clinical status of diseases such as disseminated histoplasmosis.

It has been reported that the symptoms of acute pulmonary histoplasmosis are fever, chills, malaise, headache, weakness, coughing, dyspnea, or chest pain with associated chest radiograph findings described as patchy pneumonia, enlarged mediastinal lymph nodes, bilateral diffuse reticulonodular infiltrates, or diffuse pulmonary infiltrates (1, 13, 14). Flu-like symptoms such as fever, headache, or muscle pain were seen in all patients, in addition to multiple small nodules on bilateral lungs observed on chest images. Therefore, the symptoms and signs in this report were consistent with acute pulmonary histoplasmosis. All three patients in this study recovered from the disease without specific chemotherapy for histoplasmosis and the immune status of the hosts was likely the major contributing factor for the complete control and recovery. Chest CT

scans for one of the patients showed an interesting dynamic state where most of the nodules were absent at one time but reappeared approximately one month later. Although the reason for this is unclear, we speculate that this phenomenon was due to the relationship between the pathogen and the host immune status. Furthermore, although one patient was suspected of disseminated histoplasmosis, all three cases could be considered as acute pulmonary histoplasmosis.

Generally, therapeutic guidelines for histoplasmosis state that acute self-limited syndromes and acute pulmonary histoplasmosis with mild-to-moderate illness are not indications for treatment and these cases should be closely observed (15). However, it is also recommended that treatment with itraconazole for 6-12 weeks should be considered for acute pulmonary histoplasmosis patients who have shown no clinical improvement after one month of observation. For moderate or severe acute pulmonary histoplasmosis cases, treatment with amphotericin B plus methylprednisolone is recommended. Treatment with an anti-fungal agent such as amphotericin B or itraconazole is suggested for treatment of all patients with chronic pulmonary histoplasmosis and disseminated histoplasmosis (15). Considering these therapeutic guidelines, chemotherapy might have been required for the 27-year-old patient because CT images had revealed the return of multiple nodules in bilateral lungs and *Histoplasma* DNA had been detected in her serum by PCR. Since all three patients had no underlying diseases or immunosuppressive factors, and they also showed a good clinical course, close observation was considered appropriate care. Thus far, these patients have never had recurrence of histoplasmosis, even without the use of anti-fungal agents. However, careful continued observations will be necessary for all cases in this report.

To date, the number of histoplasmosis infections in Japan is still relatively small compared with endemic countries such as the United States. As the population is increasingly mobile and able to reach anywhere in the world within 24 hours, it is important that there is awareness of the diagnosis and care of histoplasmosis patients who have traveled abroad, especially to endemic areas.

**Acknowledgement**

The authors thank Prof. Koya Ariyoshi, Institute of Tropical Medicine, Nagasaki University, for his contributions for the diagnosis of the patient, and also thank Mrs. Yuki Utena, Department of Chemotherapy and Mycoses, National Institute of Infectious Diseases, for her helpful laboratory work. A part of this report was supported by a Health Science Research Grant for "Research on Emerging and Re-emerging Infectious Diseases (H19-Sinko-Ippan-008)" from the Ministry of Health, Labor, and Welfare of Japan.

## References

1. Hage CA, Wheat LJ. Histoplasmosis. In: Harrison's Principles of Internal Medicine. 17th ed. McGraw-Hill, 2008: 1244.
2. Kamei K, Sano A, Kikuchi K, et al. The trend of imported mycoses in Japan. J Infect Chemother **9**: 16-20, 2003.
3. Centers for Disease Control and Prevention (CDC). Outbreak of histoplasmosis among travelers returning from El Salvador—Pennsylvania and Virginia, 2008. MMWR Morb Mortal Wkly Rep **57**: 1349-1353, 2008.
4. Taylor ML, Ruíz-Palacios GM, del Rocío Reyes-Montes M, et al. Identification of the infectious source of an unusual outbreak of histoplasmosis, in a hotel in Acapulco, state of Guerrero, Mexico. FEMS Immunol Med Microbiol **45**: 435-441, 2005.
5. Chamany S, Mirza SA, Fleming JW, et al. A large histoplasmosis outbreak among high school students in Indiana, 2001. Pediatr Infect Dis J **23**: 909-914, 2004.
6. Morse DL, Gordon MA, Matte T, Eadie G. An outbreak of histoplasmosis in a prison. Am J Epidemiol **122**: 253-261, 1985.
7. Hatakeyama S, Kashiyama T, Takechi A, et al. Cave-associated acute pulmonary histoplasmosis in two Japanese returning from Mexico. Nihon Kokyuki Gakkai Zasshi **39**: 293-297, 2001 (in Japanese).
8. Suzaki A, Kimura M, Kimura S, et al. An outbreak of acute pulmonary histoplasmosis among travelers to a bat-inhabited cave in Brazil. Kansenshogaku Zasshi **69**: 444-449, 1995 (in Japanese).
9. Tokimatsu I, Tashiro T, Nasu M. Early diagnosis and monitoring of human cytomegalovirus pneumonia in patients with adult T-cell leukemia by DNA amplification in serum. Chest **107**: 1024-1027, 1995.
10. de Matos Guedes HL, Guimaraes AJ, de Medeiros Muniz M, et al. PCR assay for identification of *Histoplasma capsulatum* based on the nucleotide sequence of the M antigen. J Clin Microbiol **41**: 535-539, 2003.
11. Medical Mycology Research Center, Chiba University. The trend of imported mycoses in Japan. date retrieved: July 2009 http://www.pf.chiba-u.ac.jp/ (in Japanese).
12. Wheat LJ. Current diagnosis of histoplasmosis. TRENDS in Microbiology **11**: 488-494, 2003.
13. Kauffman CA. Histoplasmosis: a clinical and laboratory update. Clin Microbiol Rev **20**: 115-132, 2007.
14. McAdams HP, Rasado-de-Christenson ML, Lesar M, et al. Thoracic mycoses from endemic fungi: radiologic-pathologic correlation. RadioGraphics **15**: 255-270, 1995.
15. Wheat J, Freifeld AG, Kleiman MB, et al. Clinical practice guidelines for the management of patients with Histoplasmosis: 2007 update by the Infectious Diseases Society of America. Clin Infect Dis **45**: 807-825, 2007.

EUKARYOTIC CELL, July 2007, p. 1150–1165 Vol. 6, No. 7
1535-9778/07/$08.00+0 doi:10.1128/EC.00091-07


# Characterization of Three Classes of Membrane Proteins Involved in Fungal Azole Resistance by Functional Hyperexpression in *Saccharomyces cerevisiae*[▽]

Erwin Lamping,[1] Brian C. Monk,[1] Kyoko Niimi,[1] Ann R. Holmes,[1] Sarah Tsao,[1]† Koichi Tanabe,[2] Masakazu Niimi,[2] Yoshimasa Uehara,[2] and Richard D. Cannon[1]*

*Department of Oral Sciences, University of Otago, Dunedin, New Zealand,[1] and Department of Bioactive Molecules, National Institute of Infectious Diseases, Tokyo, Japan[2]*

Received 20 March 2007/Accepted 10 May 2007

**The study of eukaryotic membrane proteins has been hampered by a paucity of systems that achieve consistent high-level functional protein expression. We report the use of a modified membrane protein hyperexpression system to characterize three classes of fungal membrane proteins (ABC transporters Pdr5p, CaCdr1p, CaCdr2p, CgCdr1p, CgPdh1p, CkAbc1p, and CneMdr1p, the major facilitator superfamily transporter CaMdr1p, and the cytochrome P450 enzyme CaErg11p) that contribute to the drug resistance phenotypes of five pathogenic fungi and to express human P glycoprotein (HsAbcb1p). The hyperexpression system consists of a set of plasmids that direct the stable integration of a single copy of the expression cassette at the chromosomal *PDR5* locus of a modified host *Saccharomyces cerevisiae* strain, ADΔ. Overexpression of heterologous proteins at levels of up to 29% of plasma membrane protein was achieved. Membrane proteins were expressed with or without green fluorescent protein (GFP), monomeric red fluorescent protein, His, FLAG/His, Cys, or His/Cys tags. Most GFP-tagged proteins tested were correctly trafficked within the cell, and His-tagged proteins could be affinity purified. Kinetic analysis of ABC transporters indicated that the apparent $K_m$ value and the $V_{max}$ value of ATPase activities were not significantly affected by the addition of His tags. The efflux properties of seven fungal drug pumps were characterized by their substrate specificities and their unique patterns of inhibition by eight xenobiotics that chemosensitized *S. cerevisiae* strains overexpressing ABC drug pumps to fluconazole. The modified hyperexpression system has wide application for the study of eukaryotic membrane proteins and could also be used in the pharmaceutical industry for drug screening.**

The resolution and exploitation of protein structure and function are among the greatest biological challenges in the postgenomic era. These challenges, and their potential dividends, are greatest for membrane proteins, which are notoriously difficult to functionally express and purify in the quantities and forms needed for drug discovery or for high-resolution X-ray crystallography (1, 16). About a quarter of the cellular proteome consists of membrane proteins (5), which often play vital physiological roles: from environmental sensing to energy transduction, from nutrient uptake to drug efflux, and from cellular proliferation to programmed cell death. Membrane proteins are involved in many prominent diseases, including cystic fibrosis (48), type 2 diabetes (49), heart disease (52), and the drug resistance of numerous cancers (57). Hence, they are the targets for many therapies and constitute up to 70% of the drug targets used in medicine today. Membrane proteins also play key roles in drug modification, detoxification, and resistance in a wide variety of prokaryotic and eukaryotic systems (7). A fundamental understanding of cell biology, cell physiology, and cell-drug interactions therefore requires a detailed analysis of membrane protein function. Furthermore, the development of new drugs needs both the presentation of membrane protein targets in suitable screening systems and the high-resolution structures of membrane proteins for the implementation of structure-directed drug design and virtual screening regimes. While thousands of unique high-resolution protein structures are deposited in databases, less than 0.3% of these are for membrane proteins (http://www.mpibp-frankfurt.mpg.de/michel/public/memprotstruct.html and http://blanco.biomol.uci.edu/membrane_proteins_xtal.html). In addition to requiring specialist techniques for the solubilization and purification of membrane proteins, most of the membrane protein structures resolved thus far have been obtained for proteins that are naturally highly expressed. In contrast, the vast majority of membrane proteins are expressed at low levels. Of the ~80 unique membrane protein structures obtained to date, about 75% are from bacteria and only 3 of the ~20 structures obtained for eukaryotic membrane proteins have been obtained through heterologous expression. Overcoming this well-recognized structural analysis bottleneck requires heterologous expression systems that can deliver 10- to 100-mg quantities of functional, monodisperse eukaryotic membrane proteins with minimized microheterogeneity that are suitable for crystallography (16).

Resistance of the pathogenic fungus *Candida albicans* to the azole antifungals has been shown to involve three classes of membrane protein: ATP-binding cassette (ABC) pumps, major facilitator superfamily (MFS) pumps, and overexpression and mutation of the cytochrome P450 drug target Erg11p (2,

* Corresponding author. Mailing address: Department of Oral Sciences, University of Otago, P.O. Box 647, Dunedin 9054, New Zealand. Phone: 64 3 479 7081. Fax: 64 3 479 7078. E-mail: richard.cannon@otago.ac.nz.

† Present address: Institut de Recherche en Immunologie et en Cancérologie (IRIC), Université de Montréal, Québec, Canada.

▽ Published ahead of print on 18 May 2007.

TABLE 1. Fungal and yeast strains used in this study

| Strain | Genotype or description | Source or reference |
|---|---|---|
| *Candida albicans* strain ATCC 10261 | Wild-type isolate | ATCC collection |
| *Candida glabrata* strain CBS138 | Database strain | 15 |
| *Candida krusei* strain B2399 | Wild-type isolate | CDC |
| *Cryptococcus neoformans* strain CDC551 | Serotype A, sexual type α | Chiba University, Japan |
| *Saccharomyces cerevisiae* strain AD124567 | MATα *PDR1–3 ura3 his1 Δyor1::hisG Δsnq2::hisG Δpdr10::hisG Δpdr11::hisG Δycf1::hisG Δpdr3::hisG* | 13 |
| AD1-8u$^-$ | AD124567 *Δpdr5::hisG Δpdr15::hisG* | 13 |
| ADΔ | AD1-8u, *Δura3* | This study |
| AD/ScPDR5 | AD1-8u$^-$ *Δpdr5*::pABC3-ScPDR5 | This study |
| AD/ScPDR5-HIS | AD1-8u$^-$, *Δpdr5*::pABC5′-ScPDR5-HIS | This study |
| AD/ScPDR5-GFP | AD1-8u$^-$, *Δpdr5*::pABC3-ScPDR5-GFP | This study |
| ADΔ/CaCDR1A | ADΔ, *Δpdr5*::pABC3-CaCDR1A | This study |
| AD/CaCDR1B | AD1-8u$^-$, *Δpdr5*::pABC3-CaCDR1B | 26 |
| ADΔ/CaCDR1A-HIS | ADΔ, *Δpdr5*::pABC3-CaCDR1A-HIS | This study |
| ADΔ/CaCDR1A-CYS | ADΔ, *Δpdr5*::pABC3-CaCDR1A-CYS | This study |
| ADΔ/CaCDR1A-HIS-CYS | ADΔ, *Δpdr5*::pABC3-CaCDR1A-HIS-CYS | This study |
| ADΔ/CaCDR1A-FLAG-HIS | ADΔ, *Δpdr5*::pABC3-CaCDR1A-FLAG-HIS | This study |
| ADΔ/CaCDR1A-GFP | ADΔ, *Δpdr5*::pABC3-CaCDR1A-GFP | This study |
| ADΔ/CaCDR1A-mRFP | ADΔ, *Δpdr5*::pABC3-CaCDR1A-mRFP | This study |
| AD/CaCDR2A | AD1-8u$^-$, *Δpdr5*::pABC3-CaCDR2A | 26 |
| AD/CaCDR2A-HIS | AD1-8u$^-$, *Δpdr5*::pABC5′-CaCDR2A-HIS | This study |
| AD/CaCDR2A-GFP | AD1-8u$^-$, *Δpdr5*::pABC3-CaCDR2A-GFP | This study |
| AD/CaMDR1A | AD1-8u$^-$, *Δpdr5*::pABC3-CaMDR1A | This study |
| AD/CaMDR1A-GFP | AD1-8u$^-$, *Δpdr5*::pABC5′-CaMDR1A-GFP | This study |
| AD/CaERG11A | AD1-8u$^-$, *Δpdr5*::pABC3-CaERG11A | This study |
| AD/CaERG11A-GFP | AD1-8u$^-$, *Δpdr5*::pABC5′-CaERG11A-GFP | This study |
| AD/CgCDR1 | AD1-8u$^-$, *Δpdr5*::pSK-PDR5-PPUS-CgCDR1 | 61 |
| AD/CgCDR1-HIS | AD1-8u$^-$, *Δpdr5*::3′pABC5′-CgCDR1-HIS | This study |
| AD/CgCDR1-GFP | AD1-8u$^-$, *Δpdr5*::3′pABC3-CgCDR1-GFP | This study |
| AD/CgPDH1 | AD1-8u$^-$, *Δpdr5*::pSK-PDR5-PPUS-CgPDH1 | 61 |
| AD/CgPDH1-HIS | AD1-8u$^-$, *Δpdr5*::3′pABC5′-CgPDH1-HIS | This study |
| AD/CgPDH1-GFP | AD1-8u$^-$, *Δpdr5*::3′pABC3-CgPDH1-GFP | This study |
| ADΔ/CkABC1g | ADΔ, *Δpdr5*::pABC3-CkABC1g | This study |
| ADΔ/CkABC1g-HIS | ADΔ, *Δpdr5*::pABC5′-CkABC1g-HIS | This study |
| ADΔ/CkABC1g-GFP | ADΔ, *Δpdr5*::pABC3-CkABC1g-GFP | This study |
| AD/CneMDR1 | AD1-8u$^-$, *Δpdr5*::pABC3-CneMDR1 | This study |
| AD/CneMDR1-HIS | AD1-8u$^-$, *Δpdr5*::pABC5′-CneMDR1-HIS | This study |
| AD/CneMDR1-GFP | AD1-8u$^-$, *Δpdr5*::pABC3-CneMDR1-GFP | This study |
| AD/HsABCB1 | AD1-8u$^-$, *Δpdr5*::pABC3-HsABCB1 | This study |
| AD/HsABCB1-GFP | AD1-8u$^-$, *Δpdr5*::pABC5′-HsABCB1-GFP | This study |

47, 51, 63). The development of strategies to combat the azole resistance of fungal pathogens would be facilitated greatly by studying the structures and functions of these membrane proteins. We have further developed a system for expressing membrane proteins in the yeast *Saccharomyces cerevisiae* (36, 38) and used it to study membrane proteins involved in fungal azole resistance. *S. cerevisiae* has many advantages over other expression systems as a robust eukaryotic host for membrane protein expression (5, 46). It is the best-characterized model eukaryotic organism. It can be cultured on both a micro and industrial scale, including formats suitable for protein production and drug screening, at a fraction of the cost of insect or mammalian cells, and it is readily genetically manipulated to incorporate desirable features into individual proteins or expression pathways (5, 20, 55). We previously described an *S. cerevisiae* expression system (36, 38) that utilizes a host strain deleted in several ABC transporters (13). This system has been used by us and others to heterologously express and study fungal proteins involved in drug efflux (26, 36, 38, 41, 43, 50, 54). We report here development of the system to facilitate the cloning of membrane protein genes with and without affinity, epitope, or reporter tags.

The modified *S. cerevisiae* membrane protein hyperexpression system resulted in reproducible, constitutive functional expression of fungal membrane proteins. We demonstrate that the system is well suited for the production of large quantities of membrane proteins for structural and functional studies and that yeast expressing heterologous membrane proteins can be used to screen for compounds that overcome fungal drug resistance.

## MATERIALS AND METHODS

**Strains and culture conditions.** The fungal isolates and yeast strains used in this study are listed in Table 1. All *S. cerevisiae* strains created in this study were based on AD1-8u$^-$ (13, 38). Strain ADΔ is identical to strain AD1-8u$^-$ except that the entire chromosomal *URA3* locus, which corresponds to the *URA3* marker of plasmid pABC3, was deleted by replacing the *ura3* gene of strain AD1-8u$^-$ with the 422-bp repeat region of the Ca*URA3* blaster cassette (Table 1) (64). All fungal strains were grown in yeast extract, peptone, and glucose (YPD) medium: 1% (wt/vol) Bacto-yeast extract (Difco Laboratories, Detroit, MI), 2% (wt/vol) Bacto-peptone (Difco), and 2% (wt/vol) glucose. Yeast trans-

TABLE 2. Plasmids used in this study

| Plasmid | Description | Source |
|---|---|---|
| pABC3 | Empty expression vector | This study |
| pABC3-HIS | Vector pABC3 containing a C-term. hexahistidine affinity tag | This study |
| pABC3-CYS | pABC3 containing a C-terminal tetracysteine tag | This study |
| pABC3-HIS-CYS | pABC3 containing a C-terminal tandem tag (hexa-histidine and tetra-cysteine) | This study |
| pABC3-FLAG-HIS | pABC3 containing a C-terminal tandem tag (FLAG and hexa-histidine tag) | This study |
| pABC3-GFP | pABC3 containing C-terminal YEGFP3 | This study |
| pABC3-mRFP | pABC3 containing C-terminal mRFP1 | This study |
| pABC5' | Identical to pABC3 but contains *HIS1* instead of *URA3* | This study |
| pABC5'-HIS | Identical to pABC3-HIS but contains *HIS1* instead of *URA3* | This study |
| pABC5'-CYS | Identical to pABC3-CYS but contains *HIS1* instead of *URA3* | This study |
| pABC5'-HIS-CYS | Identical to pABC3-HIS-CYS but contains *HIS1* instead of *URA3* | This study |
| pABC5'-FLAG-HIS | Identical to pABC3-FLAG-HIS but contains *HIS1* instead of *URA3* | This study |
| pABC5'-GFP | Identical to pABC3-GFP but contais *HIS1* instead of *URA3* | This study |
| pABC5'-mRFP | Identical to pABC3-mRFP but contains *HIS1* instead of *URA3* | This study |
| pABC5'-ScPDR5 | pABC3 with *PDR5* ORF from *Saccharomyces cerevisiae* AD1-8u$^-$ | This study |
| pABC3-CaCDR1A | pABC3 with A allele of *CDR1* ORF from *Candida albicans* strain 10261 | This study |
| pABC3-CaCDR1A-HIS | pABC3-HIS with A allele of *CDR1* ORF from *Candida albicans* strain 10261 | This study |
| pABC3-CaCDR1A-CYS | pABC3-CYS with A allele of *CDR1* ORF from *Candida albicans* strain 10261 | This study |
| pABC3-CaCDR1A-HIS-CYS | pABC3-HIS-CYS with A allele of *CDR1* ORF from *Candida albicans* strain 10261 | This study |
| pABC3-CaCDR1A-FLAG-HIS | pABC3-FLAG-HIS with A allele of *CDR1* ORF from *Candida albicans* strain 10261 | This study |
| pABC3-CaCDR1A-GFP | pABC3-GFP with A allele of *CDR1* ORF from *Candida albicans* strain 10261 | This study |
| pABC3-CaCDR1A-mRFP | pABC3-mRFP with A allele of *CDR1* ORF from *Candida albicans* strain 10261 | This study |
| pABC3-CaCDR1B | pABC3 with B allele of *CDR1* ORF from *Candida albicans* strain 10261 | This study |
| pABC3-CaCDR2A | pABC3 with A allele of *CDR2* ORF from *Candida albicans* strain 10261 | This study |
| pABC3-CaMDR1A | pABC3 with A allele of *MDR1* ORF from *Candida albicans* strain 10261 | This study |
| pABC3-CaERG11A | pABC3 with A allele of *ERG11* ORF from *Candida albicans* strain 10261 | This study |
| pABC3-CneMDR1 | pABC3 with *MDR1* ORF from *Cryptococcus neoformans* strain CDC551 | This study |
| pABC3-HsABCB1 | pABC3 with Hs*ABCB1* ORF from *Homo sapiens* | This study |

formants were selected on plates containing complete supplement medium without uracil (CSM−ura) (Bio 101, Vista, CA) or histidine (CSM−his; Bio 101), 0.67% (wt/vol) yeast nitrogen base without amino acids (Difco), 2% (wt/vol) glucose, and 2% (wt/vol) agar (Difco). Plasmids were maintained in *Escherichia coli* strain DH5α. *E. coli* cells were grown in Luria-Bertani medium to which ampicillin was added (100 μg/ml) as required.

**Materials.** Molecular biology reagents and restriction and modifying enzymes were from New England Biolabs (Beverly, MA) or from Roche Diagnostics N.Z. Ltd. (Auckland, New Zealand). High-performance liquid chromatography-purified DNA oligonucleotides were purchased from Hermann GbR Synthetische Biomoleküle (Denzlingen, Germany). PCR and DNA fragments were purified using kits from Qiagen Pty. Ltd. (Clifton Hill, Victoria, Australia). Genomic DNA (gDNA) was isolated from yeast using the Y-DER yeast DNA extraction reagent kit from Pierce (Rockford, IL) by downscaling 50-fold. Yeast were transformed using the alkali cation yeast transformation kit from Bio 101. A modified protocol took into account the sensitivity of strains AD1-8u$^-$ and ADΔ to high concentrations of $Li^+$ cations. A log-phase YPD culture of 250 ml (instead of 50 ml) was harvested at an optical density at 600 nm ($OD_{600}$) of 0.6 and the washed cells incubated with the $Li^+$ cation solution for only 25 min at 30°C. All plasmids and DNA fragments were verified by DNA sequencing using the DYEnamic ET Terminator cycle sequencing kit, version 3.1 (Amersham Pharmacia Biotech), and analyzed at the Micromon DNA Sequencing Facility (Monash University, Melbourne, Australia). PCRs used the high-fidelity $KOD^+$ DNA polymerase (Toyobo, Osaka, Japan, or Novagen, San Diego, CA). Site-directed mutagenesis was carried out using the Chameleon site-directed mutagenesis kit (Stratagene, La Jolla, CA).

**Compounds.** Fluconazole (FLC) (Diflucan; aqueous solution) was purchased from Pfizer Laboratories Ltd. (Auckland, New Zealand), itraconazole (ITC) and ketoconazole (KTZ) were purchased from Janssen-Kyowa (Tokyo, Japan), aureobasidin A was purchased from Takara Bio Inc. (Shiga, Japan), miconazole (MCZ), rhodamine 6G (R6G), nystatin (NYS), cycloheximide, cerulenin, enniatin, vanadate, and oligomycin were purchased from Sigma-Aldrich New Zealand Ltd. (Auckland, New Zealand), FK506 was a gift from Astellas Pharma Inc. (Tokyo, Japan), and the milbemycins α11, α20, α25, β9 and β11 were a gift from Sankyo Co. Ltd. (Tokyo, Japan).

**Construction of plasmids.** Plasmids used in this study are listed in Table 2. pABC3 was constructed from the pBluescript SK(+) (Stratagene, La Jolla, CA) derivative pSK-PDR5PPUS (38). To ensure the efficient termination of highly expressed genes, the *S. cerevisiae PGK1* transcription terminator was PCR amplified as a HindIII/BamHI fragment from gDNA and used to replace the HindIII/BamHI fragment of pSK-PDR5PPUS at a site immediately 3′ of the *PDR5* promoter sequence. PacI and NotI sites were introduced 5′ to the terminator and AscI sites introduced at each end of the transformation cassette by site-directed mutagenesis (Fig. 1A). DNA encoding a modified version of the green fluorescent protein (GFP) from *Aequorea victoria* (yEGFP3; a gift of B. P. Cormack [11]) or the monomeric red fluorescent protein (mRFP) from *Discosoma* coral (mRFP1; a gift of R. Y. Tsien [9]) was PCR amplified using 5′ primers containing NotI sites just upstream of the ATG start codon and 3′ primers containing EagI sites downstream of the reporter gene stop sequence TAA AT and directionally cloned into the pABC3 NotI site. Sequences encoding hexahistidine (His) or tetracysteine (Cys) or the double-affinity tags FLAG/His and His/Cys were ligated into the NotI site of pABC3 as double-stranded molecules obtained by annealing complementary synthetic primers which contained the tag sequence followed by the same TAA AT sequence and giving 5′ NotI- and 3′ EagI-compatible overhangs. Plasmid constructs containing the NotI site immediately upstream of the coding sequence of GFP, mRFP, or the tag sequences were selected and confirmed by DNA sequencing.

An identical set of plasmids was engineered to contain the *HIS1* auxotrophic marker (including 973 bp upstream and 378 bp downstream of the open reading frame [ORF]) instead of the *URA3* marker of vector pABC3. This series of vectors was named pABC5′ and pABC5′-tag by analogy to the pABC3 series of vectors (Fig. 1A). The parental pABC5 plasmid included a second PacI site within the *HIS1* promoter that was destroyed to facilitate directional cloning of ORFs as PacI/NotI fragments. Vector pABC5 was partially digested with PacI, and the full-length fragment was blunt ended with T4 DNA polymerase, gel purified, and religated to form pABC5′. The deletion of the PacI site in the *HIS1* promoter of plasmid pABC5′ was confirmed by DNA sequence analysis and did not affect its function.

**Construction of yeast strains overexpressing heterologous membrane proteins.** Recombinant pABC3, pABC5′, or tagged plasmids containing heterologous ORFs (2 μg) were digested with AscI and the gel-purified transformation cassette used to transform the AD1-8u$^-$ or ADΔ strain (Fig. 1A). Transformants were selected on CSM−ura or CSM−his agar plates after incubation at 30°C for 48 h to 72 h. About 100 transformants were usually obtained per μg of DNA. In each experiment, 10 transformants were selected and tested by colony PCR for the proper integration of the complete transformation cassette at the chromo-

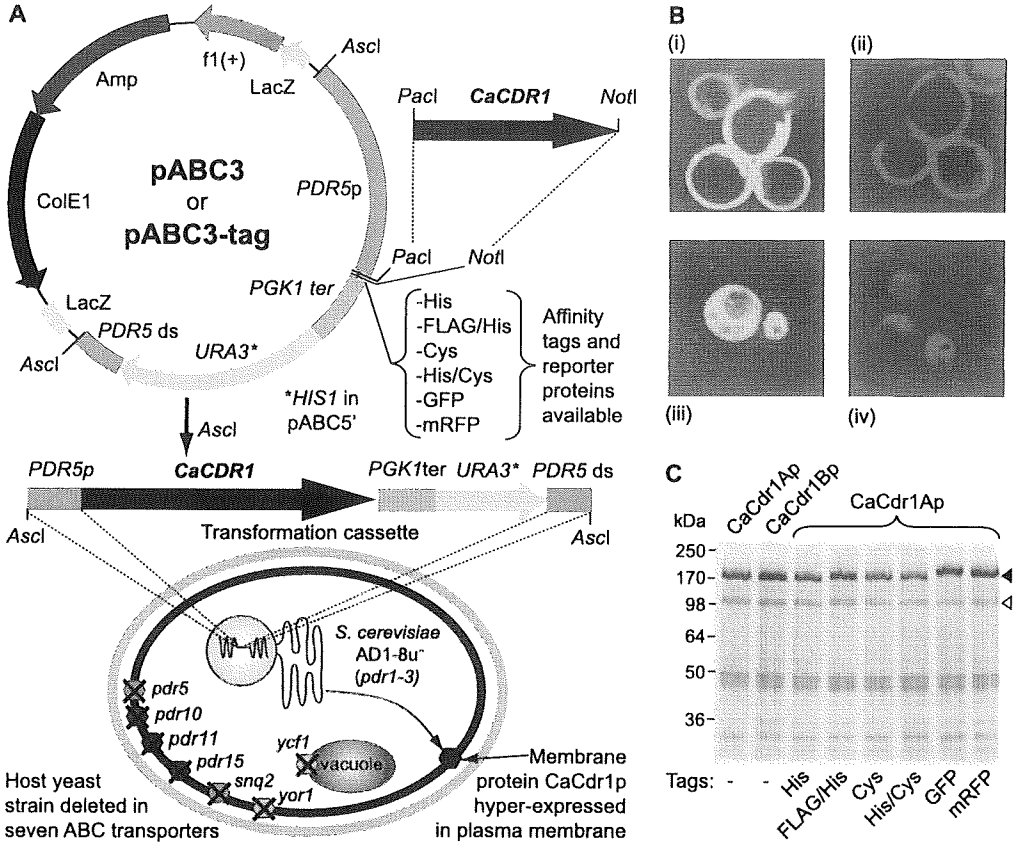


FIG. 1. (A) Schematic diagram of the yeast membrane protein hyperexpression system. The system comprises a set of vectors based on pBluescript SK(+), containing a transformation cassette that consists of the *PDR5* promoter (dark blue), the *PGK1* terminator (green), a selection marker (light blue) (*URA3* [pABC3 series of vectors] or *HIS1* [pABC5′ series of vectors]), and a small part of the 3′ end of the *PDR5* gene (dark blue). Unique 8-bp PacI and NotI cloning sites are located between the *PDR5* promoter and the *PGK1* terminator for the directional cloning of any ORF. Plasmids pABC3 and pABC5′ provided templates for derivative plasmids that contain a choice of six different C-terminal tags located 3′ to the NotI cloning site (pABC3-tag and pABC5′-tag). The transformation cassette containing an ORF cloned into the PacI and NotI sites can be excised as an AscI fragment and used to transform the host strain AD1-8u⁻. (B) Confocal microscopy images of AD1-8u⁻ cells overexpressing either the azole drug pump CaCdr1p (i and ii) or the cytosolic protein CaUra3p (iii and iv) tagged with either green (GFP) (i and iii) or red (mRFP) (ii and iv) fluorescent protein. (C) PM proteins (30 μg per lane) of AD1-8u⁻ cells hyperexpressing CaCdr1Ap, CaCdr1Bp, or CaCdr1Ap C-terminally tagged with each of the six tags were separated by SDS-PAGE and visualized with Coomassie blue.

somal *PDR5* locus. PCRs designed to amplify products across both the predicted 5′ and 3′ integration sites were used to verify the expected integration of the transformation cassette at the *PDR5* locus. For a clone to be selected as a positive transformant, both PCRs were required to amplify PCR fragments with sizes and sequences expected for integration via homologous double crossover as shown in Fig. 1A. More than 90% of transformants showed correct integration of the cassette. Three positive transformants for each construct were selected for further analysis. Hs*ABCB1* (*MDR1*) was cloned from cDNA contained on plasmid pMDRA1, kindly provided by K. Ueda, Kyoto University, Kyoto, Japan.

**Alternative strategies for obtaining strains overexpressing tagged membrane proteins.** A set of strains overexpressing C-terminally tagged membrane proteins in AD1-8u⁻ or ADΔ were obtained by two separate protocols using recombinant PCR (Fig. 2). Strains overexpressing ScPdr5p, CaCdr2Ap, CgCdr1p, CgPdh1p, CkAbc1p, and CneMdr1p with a C-terminal His tag were obtained by modifying yeast strains overexpressing the nontagged proteins (Fig. 2A). The overexpressing yeast strains were directly transformed with a DNA fragment that contained approximately 500 bp of the 3′ end of the ORF fused to the hexahistidine tag coding sequence (*His*), followed by the *PGK1* terminator, the *HIS1* marker, and the *PDR5* downstream region of plasmid pABC5′. The required PCR products were obtained in a two-step recombinant PCR amplification. First, the 3′ end of the ORF was amplified using ORF-containing DNA as a template (either plasmid or gDNA), an ORF-specific forward primer (25-mer) binding about 500 bp upstream of the ORF stop codon, and a reverse primer containing 16 bp of the His tag sequence (reverse complement), the NotI site, an extra C, and the last 25 bp of the ORF without the stop codon (Fig. 2A, PCR). The His tag-containing fragment from vector pABC5′-His was isolated as a NotI/AscI fragment and gel purified. Equal amounts (10 ng) of the two DNA fragments were combined and amplified by 15 cycles of recombinant PCR, using the ORF-specific forward primer and a reverse primer that binds to the 3′ end of the NotI/AscI fragment of plasmid pABC5′-His (Fig. 2A, recombinant PCR). The recombinant PCR product was used to transform the Ura⁺ His⁻ ORF-expressing *S. cerevisiae strain* to His⁺ Ura⁻. Yeast transformants with the *URA3* marker downstream of the ORF replaced by *HIS1* were selected on CSM−his plates.

Yeast strains overexpressing proteins with a C-terminal GFP tag were obtained by transforming yeast strains overexpressing the above C-terminal His-tagged proteins with a recombinant DNA fragment that contained 500 bp of the 3′ end of the ORF fused to the GFP tag, the *PGK1* terminator, the *URA3* marker, and the *PDR5* downstream region of plasmid pABC3-GFP (Fig. 2B, PCR). The reverse primers used to amplify the small 500-bp ORF-specific fragments contained (in reverse complement order) the first 16 bp of the GFP tag sequence, the NotI site, an extra C, and the last 25 bp of the ORF minus the stop codon. The GFP tag-containing fragment was isolated from vector pABC3-GFP as a NotI/AscI fragment and gel purified. The two fragments were fused and amplified by recombinant PCR (Fig. 2B, recombinant PCR). Yeast transformants with the *HIS1* marker downstream of the ORF replaced by the *URA3*-containing transformation PCR fragment were selected on CSM−ura plates.

Yeast strains overexpressing C-terminally GFP-tagged CaMdr1Ap, CaErg11Ap, and HsAbcb1p were obtained by transformation of yeast cells overexpressing

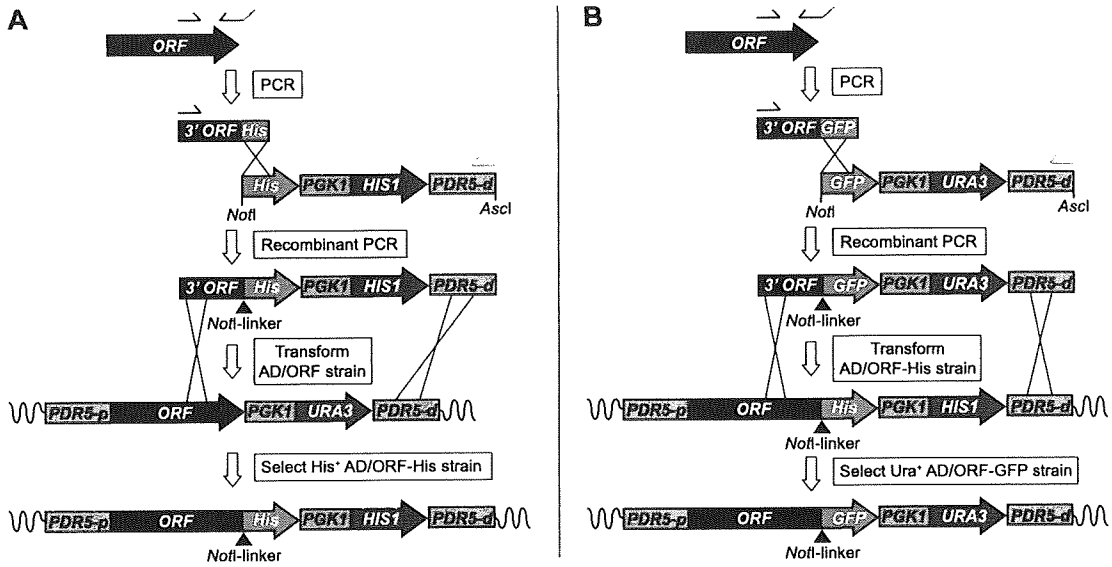


FIG. 2. Strategies for adding His or GFP tags to ORFs. (A) His tags were added by recombinant PCR, followed by transformation of *S. cerevisiae* strains already containing the heterologous ORF to His$^+$. (B) GFP tags were added by recombinant PCR, followed by transformation of *S. cerevisiae* strains already containing His tags to Ura$^+$.

nontagged protein using a recombinant PCR strategy similar to that shown in Fig. 2A. In the recombinant PCR, however, the AscI/NotI fragment of plasmid pABC5′-GFP containing the *HIS1* marker was used, and positive transformants were selected on CSM−his plates. All transformants were confirmed by colony PCR across the whole region of integration and sequencing of the resulting PCR fragments.

**Cloning of Ck*ABC1* for expression in yeast.** Because plasmid pABC3-CkABC1 could not be amplified in *E. coli*, a cloning strategy using PCR of a ligation mixture was used to clone Ck*ABC1* in *S. cerevisiae* AD1-8u$^-$. Plasmid pABC3 (10 ng) cut with PacI/NotI and 50 ng Ck*ABC1* ORF, obtained by 35 PCR cycles from genomic DNA and cut to completion with PacI/NotI, were ligated for 1 h at room temperature in a 20-μl volume using a rapid ligation protocol (Promega, Madison, WI). A 1-μl portion of the ligation mixture was then amplified in a standard 35-cycle PCR using primers that bind to the AscI regions of pABC3-CkABC1 (Fig. 1A). The resultant 7.3-kb transformation cassette was gel purified and used to transform ADΔ to Ura$^+$.

**Analysis, visualization, and purification of PM proteins.** Plasma membrane (PM) fractions of *S. cerevisiae* cells were prepared as described previously (40). Protein samples (30 μg) were separated on 8% acrylamide gels and stained with Coomassie blue R250. The relative amounts of Coomassie-stained protein bands in images of sodium dodecyl sulfate (SDS)-polyacrylamide gel electrophoresis (PAGE)-separated membrane preparations were calculated using NIH Image software. *S. cerevisiae* strains expressing GFP- or mRFP-fusion proteins were examined using a Zeiss 510 Axiovert 200 M inverted confocal laser scanning microscope (Otago Centre for Confocal Microscopy). His-tagged CaCdr1Ap was purified from PM preparations using the protocol of Ferreira-Pereira et al. (18).

**Functional analysis of membrane transporters.** The susceptibility of yeast to antifungal agents, the energy-dependent efflux of R6G from yeast cells, and the ATPase activities of PM preparations were measured as described previously (26, 40). For R6G efflux experiments, yeast cells were glucose deprived, and preloaded with 15 μM R6G, and washed. Efflux was initiated by the addition of glucose (22 mM). Agarose diffusion assays were performed to test the susceptibility of a panel of strains overexpressing drug pumps. In brief, a 10-ml YPD overnight culture of each test strain was diluted 1:20 into 3 ml CSM medium and grown at 30°C for another 4 h to mid-logarithmic growth phase ($OD_{600}$, ~1; ~$10^7$ cells/ml). The cells were diluted to an $OD_{600}$ of 0.008 in 5 ml of melted CSM containing 0.6% agarose (50°C) and plated on 20-ml CSM agarose plates. Whatman 3MM paper disks (5-mm diameter) containing xenobiotics were placed on the solidified top agarose, and the plates were incubated at 30°C for 48 h. The amounts of xenobiotics used on the disks are described in the figure legends.

**Screening for inhibitors of fungal drug pumps (chemosensitization assay).** The chemosensitization of a range of yeast strains overexpressing fungal drug pumps to FLC was carried out as described previously (40). In brief, a 10-ml YPD overnight culture of cells was diluted 1:20 into CSM and incubated at 30°C for a further 4 h. Each test strain ($OD_{600}$, ~1) was diluted to an $OD_{600}$ of 0.008 in 5 ml of melted CSM containing 0.6% agarose (50°C) with either no FLC (to determine the toxicity of each drug; control) or FLC at 0.25 × the MIC of FLC ($MIC_{FLC}$). The chemosensitizing effect of each drug was visualized at the following concentrations of FLC for each strain: AD/ScPDR5, 62.5 μg/ml; ADΔ/CaCDR1A, 50 μg/ml; AD/CaCDR2A, 15.6 μg/ml; AD/CgCDR1, 62.5 μg/ml; AD/CgPDH1, 4.0 μg/ml; ADΔ/CkABC1, 15.6 μg/ml; AD/CaMDR1A, 12.5 μg/ml. The cell suspension was poured into a rectangular Omnitray plate (126 by 86 by 19 mm; Nunc, Roskilde, Denmark) that contained 20 ml of CSM solidified with 0.6% agarose either without (control) or with 0.25× $MIC_{FLC}$. Whatman 3MM paper disks containing potential drug pump inhibitors (5 μg of milbemycins α11, α20, α25, β9, and β11, 5 μg enniatin, 25 μg FK506, or 50 nmol oligomycin) were placed on the solidified top agarose, and the plates were incubated at 30°C for 48 h.

**Nucleotide sequence accession numbers.** The DNA sequences of all 14 pABC3- and pABC5′-derived vectors shown in Fig. 1A were confirmed by DNA sequence analysis and submitted to the GenBank database (accession numbers DQ903883 to DQ903896).

## RESULTS

**Versatile yeast membrane protein hyperexpression system.** The membrane protein hyperexpression system consists of plasmids pABC3 and pABC5′, and their derivative plasmids, and the host *S. cerevisiae* strains AD1-8u$^-$ and its close relative ADΔ (see Materials and Methods) (Fig. 1A; Tables 1 and 2) (36). Both strains are deleted in seven genes encoding ABC transporters and the gene for the Pdr3p transcription factor but contain the gain-of-function mutant transcription factor Pdr1-3p (38). ABC transporters constitute one of the largest protein families known and are involved in many cellular processes, including lipid translocation and the transport of a variety of compounds across biological membranes (8, 35, 66). The lack of the seven ABC

transporters makes strains AD1-8u$^-$ and ADΔ exquisitely sensitive to a range of xenobiotics (38). The AD1-8u$^-$ strain contains *ura3* and *his1* null alleles that permit transformation using either the *URA3* and/or *HIS1* selectable markers. The ADΔ strain had the *URA3* gene completely deleted to minimize ectopic integration of the *PDR5*-flanked cassette at the *URA3* locus and to facilitate future gene disruptions using the *URA3* blaster strategy. Additional refinements to the system included the development of pABC3 and pABC5′ variants containing affinity tags and reporter proteins (Fig. 1A). Plasmids with a hexahistidine affinity tag (His), tetracysteine affinity tag (Cys) (21, 59), or double-affinity FLAG/His (28) or His/Cys tags allow the affinity purification and chemical detection or immunodetection of heterologously hyperexpressed membrane proteins. Plasmids containing the ORFs of GFP (yEGFP3) (11) or mRFP (mRFP1) (9) provide transformation cassettes that allow the visualization of heterologous proteins in *S. cerevisiae* (Fig. 1B).

**Cloning heterologous ORFs into pABC plasmids.** ORFs to be cloned in the expression system were amplified from gDNA or first-strand cDNA by PCR using a 5′ primer containing the PacI site and a 3′ reverse primer containing the NotI site just downstream of the ORF stop codon. To achieve high levels of expression, all 5′ primers contained the PacI site 11 bp upstream of the ATG start codon, followed by AAA and then the ORF ATG start codon. This maintained the size of the 5′ untranslated region (UTR) of the *PDR5* mRNA leader sequence and, most importantly, preserved the Kozak consensus sequence for highly expressed *S. cerevisiae* genes, particularly the A at position −3. The 3′ reverse primers were designed so that the ORF sequence was followed by the stop codon sequence TAA AT to ensure efficient termination of highly expressed genes (6), followed by the NotI site. Three extra nucleotides (suitable random sequences) were added at the 5′ ends of each primer to ensure efficient cutting of the PCR-amplified ORF fragments with the PacI and NotI restriction enzymes. The general design of the 5′ and 3′ primers used to clone an ORF into pABC3 and pABC5′ comprised the 5′ primer 5′-NNN TTAATTAA AAA ATG plus the first 20 bp of the ORF and the 3′ reverse primer 5′-NNN GCGGCCGC AT TTA plus the reverse complement sequence of the last 20 bp of the ORF. Most ORFs could be amplified as PacI/NotI fragments, cut with PacI and NotI restriction enzymes, gel purified, and cloned into pABC vectors. In rare cases where the ORF contained an extra internal PacI or NotI site, the ORF fragment was first partially digested with the enzyme that cut within the ORF (e.g., PacI for *PDR5*) and then the full-length partially digested ORF fragment was gel purified and fully digested with the second enzyme before cloning into pABC3 or pABC5′ was done.

**Cloning heterologous ORFs into pABC3-tag or pABC5′-tag plasmids.** Directional cloning of ORFs as PacI/NotI fragments into any of the 12 tagged vectors required a slight modification of the 3′ reverse primer described above. The modifications included the removal of the AT TTA reverse stop codon sequence and the addition of one extra C nucleotide 3′ to the NotI site to ensure an in-frame fusion of the ORF with the chosen tag. Thus, the 3′ reverse primer sequence to PCR amplify any ORF for cloning into a tagged vector comprised 5′-NNN GCGGCCGCC plus the reverse complement sequence of the last 20 bp of the ORF (the extra C nucleotide is in bold). Cloning ORFs into pABC3-tag or pABC5′-tag vectors with these primers introduced a three-amino-acid C-terminal linker (GGC GGC CGC, encoding Gly-Gly-Arg) between the ORF and the tag.

**Cloning heterologous ORFs in *S. cerevisiae*.** ORFs encoding genes to be hyperexpressed in *S. cerevisiae* AD1-8u$^-$ or ADΔ were PCR amplified and directionally cloned into the PacI and NotI restriction sites of pABC3, pABC5′, or their derivative plasmids (see Materials and Methods) (Fig. 1A). A transformation cassette containing the inserted ORF with or without a C-terminal fusion to any of the six tags, the *S. cerevisiae PGK1* terminator, the *URA3* or *HIS1* selection marker, and flanking *PDR5* sequences was excised from the recombinant plasmid with AscI. The toxicity of plasmid pABC3-CkABC1 precluded cloning the Ck*ABC1* gene in *E. coli*. In this case, the entire transformation cassette was amplified by PCR directly from the ligation mix (see Materials and Methods). The selection of Ura$^+$ or His$^+$ transformants of AD1-8u$^-$ directs the integration of the linearized transformation cassette, via homologous recombination of its terminal sequences, at the *PDR5* chromosomal locus (Fig. 1A).

**Hyperexpression of ABC efflux pump ScPdr5p and CaCdr1p in *S. cerevisiae*.** The efficiency of the *S. cerevisiae* membrane protein hyperexpression system was demonstrated by cloning the homologous Sc*PDR5* gene into strain AD1-8u$^-$ to form AD/ScPDR5. The level of ScPdr5p expression in AD/ScPDR5 was compared to the expression of ScPdr5p in the control strain, AD124567 (13). AD124567 is a precursor to strain AD1-8u$^-$ that still contains the wild-type *PDR5* gene. SDS-PAGE analysis of PM preparations and measurement of the strains' $MIC_{FLC}$s showed that the levels of ScPdr5p expression were identical between the two strains (data not shown). This control experiment confirmed that the modifications to the 5′ and 3′ UTR of *PDR5* introduced using our simple cloning strategy (Fig. 1A) maintained the high level of protein expression achieved with the wild-type *PDR5* UTR.

The membrane protein hyperexpression system was used to study proteins involved in the FLC resistance of *Candida albicans*. This yeast is an opportunistic pathogen of the immunocompromised and can cause a range of infections in the very young, the elderly, cancer patients, organ transplant recipients, and HIV-positive/AIDS patients (45, 63). Triazole antifungals, such as FLC, which inhibit the microsomal cytochrome P450 enzyme 14α-lanosterol demethylase (Erg11p), involved in ergosterol biosynthesis, are widely used to treat candidiasis patients (63). Prolonged courses of the antifungal FLC lead to the emergence of *C. albicans* strains resistant to FLC. Low-level resistance can be due to overexpression of the drug target Erg11p or mutations in Erg11p. Higher levels of resistance correlate with overexpression of the MFS drug pump Mdr1p or the ABC pump Cdr1p or Cdr2p (2, 47, 51). *C. albicans* is diploid, and we cloned the A allele of *CDR1* of *C. albicans* strain ATCC 10261 into the PacI and NotI sites of pABC3 and transformed *S. cerevisiae* AD1-8u$^-$ with the AscI fragment of the recombinant plasmid (Fig. 1A). Hyperexpression of CaCdr1Ap in the PM (Fig. 1C) conferred on AD1-8u$^-$ resistance to the azole drugs FLC, ITC, and other azoles but not to

TABLE 3. Phenotypes conferred on *S. cerevisiae* AD1-8u$^-$ by hyperexpression of fungal drug efflux pumps and other membrane proteins

| Hyperexpressed protein | MIC of drug (μg/ml) | | | R6G efflux[a] (pmol/$10^7$ cells/min) | ATPase activity[a,b] (nmol Pi/min/mg protein) |
|---|---|---|---|---|---|
| | FLC | ITC | NYS | | |
| None (pABC3) | 0.5 | 0.031 | 2 | 0.0 | 7 ± 2 |
| ScPdr5p | 300 | >32 | 2 | 93 ± 5 | 199 ± 12 |
| CaCdr1Ap (allele A) | 200 | >32 | 2 | 75 ± 9 | 185 ± 4 |
| CaCdr1Bp (allele B) | 300 | >32 | 2 | 79 ± 7 | 188 ± 3 |
| CaCdr2Ap (allele A) | 75 | 4 | 2 | 22 ± 5 | 128 ± 9[c] |
| CaCdr2Bp (allele B) | 150 | >32 | 2 | 33 ± 3 | 164 ± 16[c] |
| CaMdr1Ap | 60 | 0.031 | 2 | 0.0 | 6 ± 2 |
| CaErg11Ap | 5 | 0.125 | 2 | 0.0 | 5 ± 2 |
| CgCdr1p | 300 | >32 | 4 | 105 ± 1 | 200 ± 14 |
| CgPdh1p | 8 | 0.062 | 4 | 15 ± 3 | 141 ± 19 |
| CkAbc1p | 32 | 8 | 2 | 82 ± 5 | 57 ± 2 |
| CneMdr1p | 5 | >32 | 2 | 92 ± 20 | 45 ± 3 |

[a] Mean ± SD for three experiments carried out in triplicate.
[b] Oligomycin (20 μM)-sensitive ATPase activity, measured at pH 7.5.
[c] Two hundred micromolar oligomycin used in assays.

the polyene NYS (Table 3 and Fig. 3), as expected, since NYS is not a substrate of ABC pumps. Some of the phenotypic effects could, however, be caused by the background mutations in host strains AD1-8u$^-$ and ADΔ. These mutations and the expression of certain pumps could potentially affect PM composition and concomitantly alter ABC pump function, thus leading to slightly changed substrate specificities that are not seen in the natural host. Allelic variation caused by single-nucleotide polymorphisms can affect gene function. The Ca*CDR1A*, Ca*CDR1B*, Ca*CDR2A*, and *CaCDR2B* alleles of *C. albicans* ATCC 10261 were individually cloned and expressed in AD1-8u$^-$ (Fig. 1C and 4C). The expression of each CaCdr1p and CaCdr2p allele to the same extent enabled identification of functional differences between each of these pairs of alleles (26) and further characterization of these proteins' functions.

To analyze the trafficking of heterologous CaCdr1Ap to the *S. cerevisiae* PM, Ca*CDR1A* was cloned in AD1-8u$^-$ fused to GFP or mRFP. When *S. cerevisiae* cells expressing these fusion proteins were grown under standard conditions, confocal microscopy indicated that the proteins were correctly trafficked to the cell surface (Fig. 1B, i and ii), which did not occur with overexpression of plasmid-encoded CaCdr1p (19). Only a minor proportion of the CaCdr1Ap protein was located in the cell interior, seemingly around the nucleus. In contrast, CaUra3p fusion proteins in control strains, created by expressing *C. albicans* ATCC 10261 *URA3* (encoding the cytoplasmic enzyme orotidine-5′-phosphate decarboxylase) in our system,

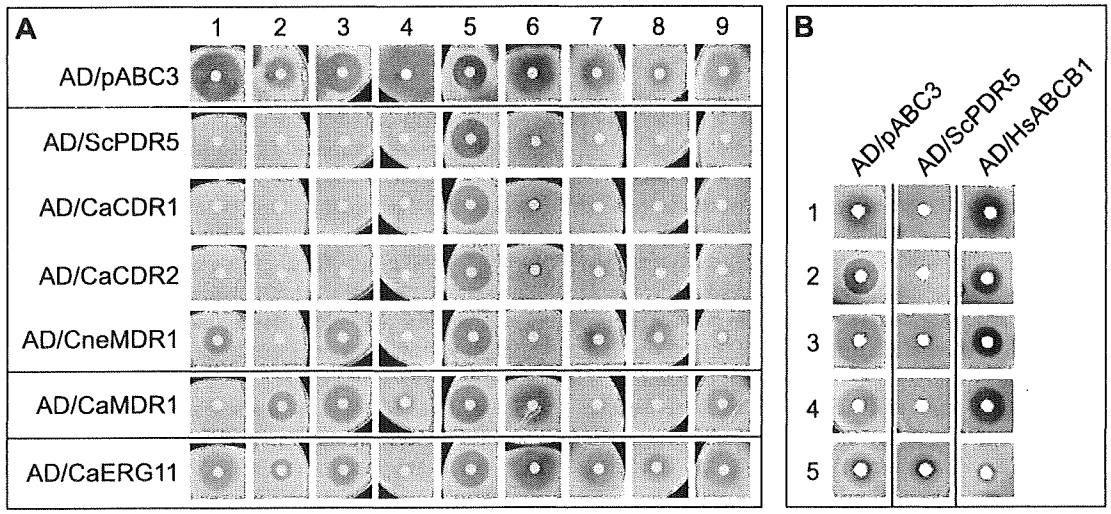


FIG. 3. Agarose diffusion assays of AD1-8u$^-$ cells overexpressing a selection of fungal ABC drug pumps (ScPdr5p, CaCdr1Ap, CaCdr2Ap, and CneMdr1p), a fungal MFS drug pump, CaMdr1Ap, the azole drug target CaErg11Ap, and the sensitive control strain AD1-8u$^-$ containing the empty pABC3 transformation cassette integrated at the chromosomal *PDR5* locus (AD/pABC3). Cells were analyzed using agarose diffusion assays as described in Materials and Methods. (A) Susceptibilities to the following xenobiotics were tested: 1, FLC (10 μg); 2, ITC (0.16 μg); 3, MCZ (0.2 μg); 4, KTZ (0.2 μg); 5, NYS (60 μg); 6, R6G (48 μg); 7, cycloheximide (0.2 μg); 8, cerulenin (1 μg); 9, Triton X-100 (1 mg). (B) As in panel A, the substrate specificities of cells overexpressing HsAbcb1p were tested and compared to those of cells overexpressing ScPdr5p using the control strain AD/pABC3. Drugs applied were as follows (top to bottom): 1, FLC (4 μg); 2, ITC (0.5 μg); 3, R6G (80 μg); 4, Triton X-100 (1 mg); 5, aureobasidin A (20 μg).

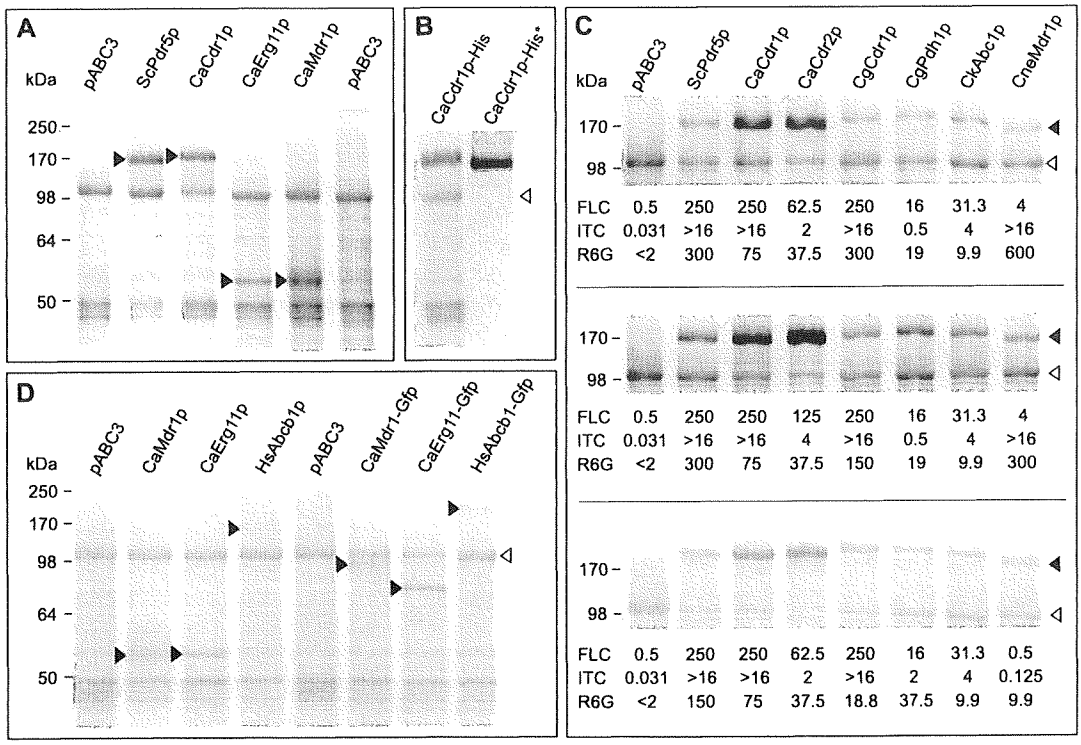


FIG. 4. SDS-PAGE analysis of PM proteins (30 μg per lane) from AD1-8u$^-$ cells overexpressing different fungal and human membrane proteins. In each panel, filled arrowheads indicate heterologous proteins and open arrowheads indicate the endogenous 100-kDa PM $H^+$ ATPase (Pma1p). (A) AD1-8u$^-$ cells overexpressing different classes of fungal membrane protein: ABC transporters ScPdr5p and CaCdr1Ap, MFS transporter CaMdr1Ap, and the azole drug target CaErg11Ap, a cytochrome $P_{450}$ enzyme. pABC3 refers to the drug-sensitive control strain as described in the legend to Fig. 3. (B) The left lane shows 30 μg of PM protein isolated from AD/CaCDR1A-His-p cells. CaCdr1A-His-p after Ni affinity chromatography is shown in the right lane. (C) Fungal drug pumps hyperexpressed in AD1-8u$^-$ cells (top panel). The addition of a C-terminal His tag (middle panel) or GFP tag (bottom panel) does not affect their level of expression. Shown below the gel in each panel are the FLC, ITC, and R6G MICs (μg/ml) for each of the overexpressing strains. (D) SDS-PAGE analysis of PM proteins isolated from AD/CaMDR1A, AD/CaERG11A, and the AD/HsABCB1 cells and their GFP-tagged derivatives.

were uniformly distributed throughout the cytoplasm and excluded from organelles (Fig. 1B, iii and iv).

The effect of tags on heterologous gene expression was investigated by cloning Ca*CDR1A* into pABC3 derivatives so that the following tags were fused to the CaCdr1Ap C terminus: His, FLAG/His, Cys, and His/Cys. None of these tags or fusion to GFP or mRFP caused a significant reduction in CaCdr1Ap expression in PM preparations (Fig. 1C). Only the Cys-containing tags (Cys and His/Cys) slightly reduced the expression of CaCdr1Ap (Fig. 1C).

**Hyperexpression and characterization of other fungal membrane proteins involved in azole resistance.** The *S. cerevisiae* membrane protein hyperexpression system was used to functionally express three classes of fungal membrane protein that are involved in resistance of *C. albicans* to FLC. Individual alleles of *C. albicans* ATCC 10261 *CDR1* (GenBank accession numbers DQ462358 and DQ462359) (26), *CDR2* (GenBank accession numbers DQ470007 and DQ470008) (26), *ERG11* (GenBank accession number DQ903897), and *MDR1* (GenBank accession number DQ903899) were cloned and expressed in *S. cerevisiae* AD1-8u$^-$. SDS-PAGE analysis of recombinant *S. cerevisiae* strains indicated that polypeptides of the expected molecular masses were hyperexpressed in PM fractions (Fig. 4). The identity of the hyperexpressed protein could be confirmed for CaCdr1Ap, CaCdr2Ap, and CaMdr1Ap by immunodetection (26, 38) and for CaErg11Ap and ScPdr5p by mass spectrometry of tryptic fingerprints (data not shown). The expression of these proteins, measured by NIH Image analysis of Coomassie blue-stained SDS-PAGE profiles, ranged from 29% (for CaCdr1Ap) to 4.9% (for Erg11Ap) of PM protein. The hyperexpressed membrane proteins were shown to be functional with three assays of whole-cell or in vitro function: antifungal susceptibility, energy-dependent efflux of the fluorescent pump substrate R6G, and ATPase activity. The host strain AD1-8u$^-$ is hypersusceptible to the triazole antifungals FLC and ITC (Table 3). Expression of CaCdr1Ap or the *S. cerevisiae* ortholog ScPdr5p increased the resistance of AD1-8u$^-$ to FLC and ITC between 400 and >1,000-fold (Table 3). Expression of the MFS membrane transporter CaMdr1Ap conferred less resistance to FLC and no resistance to ITC (Table 3; Fig. 3), as has been found for clinical *C. albicans* isolates expressing Mdr1p (47). Hyperexpression of the azole drug target CaErg11Ap conferred only a 4- to 10-fold increase in azole resistance (Table 3). Hyperexpression of fungal transporters did not confer on *S. cerevisiae* resistance to the polyene antifungal NYS, which is not a substrate for the pumps (Table 3; Fig. 3). *S. cerevisiae* cells expressing fungal ABC transporters but not the MFS pump CaMdr1Ap demonstrated R6G efflux

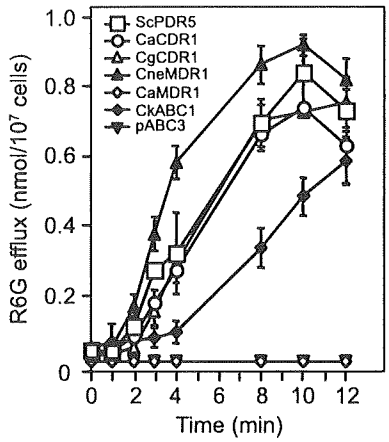


FIG. 5. In vivo pumping activities of different fungal drug pumps using the fluorescent pump substrate R6G. AD1-8u$^-$ cells overexpressing drug pumps were grown to mid-logarithmic phase, harvested, and loaded with the fluorescent substrate R6G, and the assay was started by the addition of glucose as an energy source as described in Materials and Methods. The fluorescence intensity accumulating in the supernatant after filtration of the cells was measured and the R6G pumping activity per $10^7$ cells determined. The results are the means ± standard deviations for triplicate determinations.

in a time- and energy-dependent fashion (Table 3; Fig. 5). Finally, the drug efflux pump ATPase activity of cells expressing ABC transporters was measured (Table 3). PM fractions from cells expressing ABC but not MFS pumps had significant ATPase activities. The pump ATPase activity could be distinguished from the PM $H^+$ ATPase activity because it was oligomycin sensitive and active at pH 7.5 (Fig. 6C).

**A panel of *S. cerevisiae* strains hyperexpressing fungal ABC transporters.** The hyperexpression system was used to express ABC transporters from other fungal pathogens, including the *Candida glabrata* database strain CBS138 (Cg*CDR1* and Cg*PDH1*), *Candida krusei* strain B2399 (Ck*ABC1*), and *Cryptococcus neoformans* strain CDC551 (Cne*MDR1*) (Tables 1 and 2; Fig. 4C). The AD/CgCDR1 and AD/CgPDH1 strains were described previously (61). The putative azole drug pump encoded by Ck*ABC1*, thought to be involved in the innate azole drug resistance of *C. krusei*, was originally described by Katiyar and Edlind (29). They reported the cloning of a 300-bp fragment of Ck*ABC1* corresponding to a highly conserved consensus region of ABC transporters. We used inverse PCR to clone Ck*ABC1* and discovered that the 4.65-kb Ck*ABC1* gene contains an 88-bp intron at the 5′ end of the ORF (GenBank accession numbers DQ903906 and DQ903907). A strain expressing Ck*ABC1* cDNA (AD/CkABC1-c) was created and was found to have properties similar to those of AD-CkABC1. The PM preparations from AD/CkABC1-c cells contained 50% to 100% more CkAbc1p than PM preparations from intron-containing AD/CkABC1 cells (data not shown). This indicated that although *S. cerevisiae* recognizes the Ck*ABC1* intron, its processing gave a reduced level of CkAbc1p expression. Cne*MDR1* was isolated from *C. neoformans* strain CDC551 and found to be identical to the published sequence of Cne*MDR1* isolated from a different strain (GenBank accession number DQ903909).

The overexpression of each of these fungal ABC transporters conferred increased azole drug resistance on AD1-8u$^-$ (Fig. 4C, top panel; Table 3). As expected, each transporter effluxed R6G in a time- and energy-dependent fashion, albeit at different rates and with different lag periods after the addition of glucose (Table 3; Fig. 5) (13, 26, 61, 62). These data confirmed the hypothesis that all these transporters are energy-dependent azole drug efflux pumps. There was a positive correlation between the R6G efflux activity and the resistance of strains expressing ABC transporters (apart from CneMdr1p) to FLC determined by liquid MIC measurements. All the ABC drug efflux pumps showed ATPase activity, and although activity was generally higher in strains with higher $MIC_{FLC}$s, the relationship was not linear, indicating an indirect relationship between ATPase activity and FLC susceptibility. This may reflect different degrees of coupling between energy utilization in the nucleotide binding domains and drug transport mediated by the membrane sector of the pumps (61).

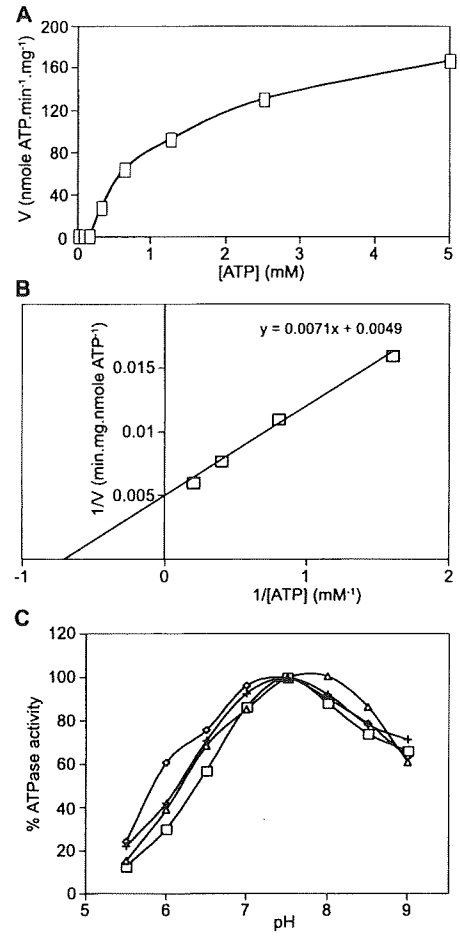


FIG. 6. Kinetic parameters for the ATPase activities of fungal ABC drug transporters. (A) Vanadate-sensitive ATPase activity (V) versus substrate concentration plot for Cdr1Ap-His/Cys-tagged drug pump at pH 7.5. (B) Lineweaver Burke plot for the vanadate-sensitive ATPase activity of the CaCdr1Ap-His/Cys-tagged drug pump at pH 7.5. The data were taken from panel A. (C) The pH profile for the ATPase activity of untagged CaCdr1Ap (diamond) or CaCdr1Ap with a His tag (square), Cys tag (triangle), or His/Cys tag (cross) is shown. Results are expressed as percentages of activity at pH 7.5.

TABLE 4. Effect of tags on pump ATPase activity and response to inhibitors

| Hyperexpressed pump | Kinetics of ATPase activity | | | $IC_{50}$ of: | | |
|---|---|---|---|---|---|---|
| | $K_{m\ app}$ (mM ATP) | $V_{max}$ (nmol/min/mg) | pH optimum | Vanadate (μM) | Oligomycin (μM) | FK506 (μg/ml) |
| None (AD1-8u$^-$) | 2.61 | 30 | 6–8 | | | |
| Sc*PDR5* | 1.42 | 303 | 7.5 | 1.3 | 0.25 | 0.013 |
| Sc*PDR5*-His | 1.30 | 333 | 7.5 | 1.3 | 0.30 | 0.013 |
| Ca*CDR1A* | 1.31 | 135 | 7.5 | 3.1 | 0.30 | 0.63 |
| Ca*CDR1A*-His | 1.20 | 133 | 7.5 | 3.1 | 0.30 | 0.63 |
| Ca*CDR1A*-Cys | 1.82 | 111 | 7.5–8.0 | 12.5 | 0.70 | 0.80 |
| Ca*CDR1A*-His-Cys | 1.45 | 204 | 7.5 | 6.3 | 0.70 | 0.60 |
| Ca*CDR2A* | 2.45 | 250 | 7.5 | 1.3 | >20 | 20 |
| Ca*CDR2A*-His | 1.05 | 278 | 7.5 | 3.0 | >20 | 20 |
| Cg*CDR1* | 1.95 | 227 | 7.5 | 1.5 | 0.063 | 0.0063 |
| Cg*CDR1*-His | 1.27 | 303 | 7.5 | 1.6 | 0.01 | 0.013 |
| Cg*PDH1* | 0.60 | 270 | 7.0 | 0.9 | 0.30 | 0.013 |
| Cg*PDH1*-His | 0.85 | 303 | 7.0 | 1.3 | 0.30 | 0.013 |
| Ck*ABC1* | 1.31 | 161 | 7.5 | 0.8 | 0.40 | 1.0 |
| Ck*ABC1*-His | 1.45 | 204 | 7.5 | 1.3 | 0.40 | 1.0 |
| Cne*MDR1* | 1.71 | 95 | 6.5–7.0 | 3.1 | 0.50 | 20 |
| Cne*MDR1*-His | 1.03 | 79 | 6.5–7.0 | 4.0 | 1.00 | 20 |

**Effect of affinity and epitope tags on membrane protein function.** The overexpression, purification, and crystallization of membrane proteins constitute a challenging scientific endeavor. Besides achieving high levels of expression, it is paramount for the crystallization of membrane proteins that the overexpressed membrane protein can be solubilized with mild detergent and remain stable in solution as a monodisperse molecule. After successful overexpression of an array of fungal membrane proteins, C-terminally hexahistidine-tagged derivatives of these fungal ABC drug pumps were created to facilitate their affinity purification. The addition of a His tag did not affect the level of overexpression of any of the seven ABC transporters tested (Fig. 4C, middle panel). Initial purification efforts using PMs obtained from ADΔ/CaCDR1A-His were very promising. CaCdr1Ap-His was readily solubilized with the mild detergent dodecylmaltoside, and a one-step nickel affinity purification led to a CaCdr1Ap-His protein fraction with greater than 95% purity (Fig. 4B).

**Effects of C-terminal affinity tags on kinetics and inhibition of fungal ABC transporter ATPase activities.** The effects of C-terminal tags on the function of fungal ABC transporters was determined by the measurement of kinetic parameters and responses to known inhibitors of their ATPase activity in PM preparations. All pumps, including those modified with C-terminal His, Cys, and His/Cys tags, showed rate-versus-ATP concentration profiles that approximated Michaelis-Menten kinetics at higher ATP concentrations. Figure 6A and B show the results for PMs containing CaCdr1pA-His/Cys as a typical example. The apparent $K_m$ ($K_{m\ app}$) values for the unmodified ABC transporters lay within a narrow range of 0.6 mM ATP for CgPdh1p to 2.45 mM ATP for CaCdr2Ap, with most ABC transporters having a $K_{m\ app}$ value of about 1.5 mM ATP. The addition of a C-terminal His tag had only minor effects on the $K_{m\ app}$ values (Table 4). At ATP concentrations at least twofold below the $K_{m\ app}$ value, all pumps showed positive cooperativity with ATP, as expected for ABC transporters with two ATP molecules in the active site (Fig. 6A). The $V_{max}$ values of ATPase activity in the PM preparations ranged between 95 nmol/min/mg for CneMdr1p and 270 nmol/min/mg for CgPdh1p among the nontagged pumps. The addition of C-terminal His tags also had only modest effects on $V_{max}$ values. The pH optimum for ScPdr5p, CaCdr1Ap, CaCdr2Ap, CgCdr1p, and CkAbc1p was 7.5, with a slight shift to neutral pH for CgPdh1p (7.0) and CneMdr1p (6.5 to 7.0). The addition of a C-terminal His tag to the ABC transporters had no effect on any of the pH profiles. For CaCdr1Ap, the influence of a C-terminal Cys tag or the double-affinity tag His/Cys on its kinetic parameters was tested. Both tags had minor effects on the $K_{m\ app}$, $V_{max}$, and pH optimum values. Most notably, a slight alkaline shift in the pH optimum was seen for the C-terminal Cys tag (7.5 to 8.0) (Fig. 6C; Table 4).

As independent measures of ABC transporter function, the 50% inhibitory concentrations ($IC_{50}$s) for known inhibitors of ATPase activity were determined. The vanadate $IC_{50}$s of all ABC transporters were within a narrow range between 0.8 μM for CkAbc1p and 3.1 μM for CneMdr1p. The addition of a C-terminal His tag hardly affected the $IC_{50}$s of vanadate for any of the pumps except for CaCdr2Ap (3.0 μM for CaCdr2Ap-His versus 1.3 μM for CaCdr2Ap). The addition of a C-terminal Cys tag led to a fourfold increase in the $IC_{50}$ for vanadate (12.5 μM for CaCdr1Ap-Cys versus 3.1 μM for CaCdr1Ap). The $IC_{50}$s for the ATPase activities of the panel of fungal ABC transporters for oligomycin and FK506 were not significantly affected by the presence of any of the tags (Table 4). With the exception of CgCdr1p, which was highly sensitive to inhibition by oligomycin ($IC_{50}$ = 0.063 μM), and CaCdr2Ap, which was poorly inhibited by oligomycin ($IC_{50}$ > 20 μM), the oligomycin $IC_{50}$s for the ABC transporters lay within a very narrow range of 0.25 μM for ScPdr5p to

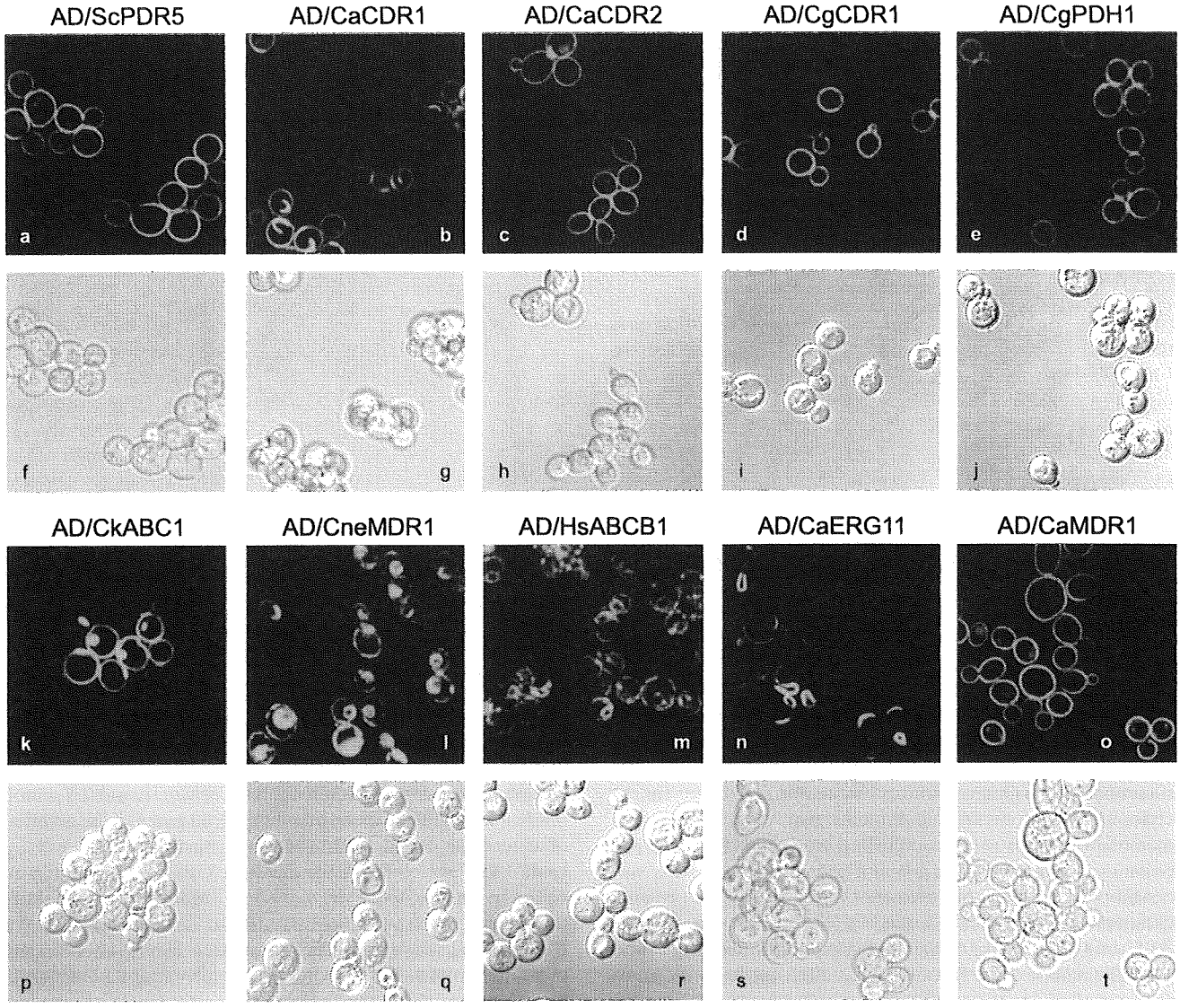


FIG. 7. Confocal microscopy images of AD1-8u$^-$ cells overexpressing different classes of membrane proteins. ABC drug pumps ScPdr5p (a), CaCdr2Ap (c), CgCdr1p (d), and CgPdh1p (e) localized exclusively to the PM, whereas the fungal drug pumps CaCdr1Ap (b) and CkAbc1p (k) also partially localized in internal membrane structures. CneMdr1p (l) and HsAbcb1p (m) were not evenly distributed throughout the PM and were also found in internal structures. The MFS drug pump CaMdr1Ap (o) localized exclusively to the PM, and the azole drug target CaErg11Ap (n) localized to the endoplasmic reticulum, as expected. Light microscopy images of the cells (f to j and p to t) are shown below their confocal images (a to e and k to o).

0.5 μM for CneMdr1p. FK506 was a very effective inhibitor of the ATPase activities of CgCdr1p ($IC_{50}$ = 0.0063 μM), CgPdh1p ($IC_{50}$ = 0.013 μM), and ScPdr5p ($IC_{50}$ = 0.013 μM). Severalfold-higher concentrations were required to inhibit CaCdr1Ap and CkAbc1p ($IC_{50}$ = 0.63 μM and 1.0 μM, respectively). FK506 was an even less effective inhibitor of the ATPase activities of CaCdr2Ap and CneMdr1p ($IC_{50}$ > 20 μM), with 200 μM FK506 required to obtain 90% inhibition (data not shown). The cross-resistance of CaCdr2p to FK506 and oligomycin was not found for CneMdr1p, indicating that the FK506 and oligomycin binding sites are not identical. In summary, apart from the Cys and His/Cys double tags, the addition of C-terminal affinity tags did not affect significantly the level of expression or the kinetic characteristics of any of the fungal ABC transporters tested. Furthermore, the addition of a C-terminal His tag also did not affect the overall function of any of these ABC transporters, as measured by their in vivo resistance to the drugs FLC, ITC, and R6G (Fig. 4C).

**Cellular location of heterologously overexpressed membrane proteins.** While the addition of a C-terminal GFP tag to any of the seven fungal ABC transporters tested did not affect their level of expression in the PM, the drug sensitivities of these yeast strains and the determination of the cellular location of the transporters by confocal microscopy indicated that in some cases, function and/or cellular localization could be affected (Fig. 4C and 7). The FLC, ITC, and R6G MICs for some strains overexpressing ABC transporters indicated that they are affected in their in vivo transport function with some but not other substrates (Fig. 4C, lower panel). The addition of

the GFP tag reduced the $MIC_{FLC}$ and $MIC_{ITC}$ for AD/CneMDR1 but not for the other six strains overexpressing fungal ABC transporters. The GFP tag had more complex effects on R6G transport. It reduced the $MIC_{R6G}$ of AD/CneMDR1 128-fold, that AD/ScPDR5 2-fold, and that of AD/CgCDR1 16-fold. The C-terminal GFP tag on CgPdh1p, however, increased the $MIC_{ITC}$ fourfold and the $MIC_{R6G}$ twofold. Confocal microscopy revealed that ScPdr5p, CaCdr2Ap, CgCdr1p, and CgPdh1p were properly and exclusively located in the PM (Fig. 7). However, a small fraction of CaCdr1Ap and CkAbc1p and the largest fraction of CneMdr1p were localized inside the cell in structures reminiscent of the endoplasmic reticulum (56). Since the C-terminal GFP tag did not increase the susceptibility of cells overexpressing CaCdr1Ap or CkAbc1p to FLC, ITC, or R6G, the confocal images of GFP-tagged proteins probably reflect the localization of the native untagged proteins. For CneMdr1p, the addition of the C-terminal GFP tag increased the susceptibilities of AD/CneMDR1 to azoles and R6G (Fig. 4C). This suggests that either the function of CneMdr1p was affected or the localization of CneMdr1p-GFP determined by confocal microscopy did not reflect the localization of nontagged CneMdr1p. CaMdr1Ap and CaErg11Ap were also labeled with a C-terminal GFP tag. CaMdr1Ap localized exclusively to the cell surface. CaErg11Ap localized primarily to the endoplasmic reticulum, as expected, with a small amount present on the cell surface. That result is consistent with CaErg11Ap being detected in the PM preparations (Fig. 4A and D). Upon closer inspection, it appeared that CaErg11Ap was also significantly concentrated in the same internal karmella-like structures (often round and sometimes hook-like structures depending on the plane of observation) that possibly surround the nucleus as described for CaCdr1Ap, CkAbc1p, CneMdr1p, and also HsAbcb1p (see below).

**Substrate specificities of overexpressed drug pumps and affinities of the azole drug target CaErg11Ap to a range of azoles.** The panel of *S. cerevisiae* strains expressing heterologous membrane proteins enabled the use of agarose diffusion assays to identify drug efflux pump substrates and compare the drug sensitivities of the azole target Erg11p. The specific overexpression of the fungal drug pumps ScPdr5p, CaCdr1Ap, and CaCdr2Ap gave reduced susceptibilities to all nine xenobiotics tested except to the negative control, NYS, indicating that the remaining eight drugs are substrates of these pumps (Fig. 3A). The overexpressed fungal efflux pumps CgCdr1p and CgPdh1p have previously been shown to confer similar phenotypes (61). In contrast, CneMdr1p pumped only ITC, KTZ, R6G, Triton X-100, and, slightly less effectively, FLC. AD/CneMDR1 remained sensitive to MCZ, cycloheximide, and cerulenin, and these drugs are therefore not substrates. Although CaMdr1p is known to confer resistance to benomyl, cycloheximide, and cerulenin (4, 24) and has been reported to pump FLC (65), we found that KTZ is also a CaMdr1p substrate (Fig. 3A). The detection of this activity may be due to the high CaMdr1p expression level achieved, or it may reflect the fact that our genetically modified host strains AD1-8u$^-$ and AD$\Delta$ are more sensitive to xenobiotics, which allows the detection of pump substrates that could not be identified using their natural hosts due to the masking of these activities by their other endogenous pumps. As expected, the overexpression of the drug target CaErg11Ap gave significantly reduced susceptibilities to different azole drugs but not to the polyene antibiotic NYS or the pump substrates R6G, cycloheximide, cerulenin, or Triton X-100 (Fig. 3A). For comparable amounts of ITC, MCZ, and KTZ, the relative sizes of the growth inhibition zones indicated that KTZ is a significantly less effective inhibitor of CaErg11Ap than either ITC or MCZ.

**Expression of human membrane protein HsAbcb1p in *S. cerevisiae*.** Human P glycoprotein (HsAbcb1p) is an ABC transporter implicated in the development of drug resistance by cancer cells that has been studied by the scientific community for three decades (22, 57). Hs*ABCB1* was successfully cloned and expressed in *S. cerevisiae* AD1-8u$^-$ (Fig. 4D). Although the expression of HsAbcb1p at 3.3% of total PM protein as measured by NIH Image software was significantly lower than that achieved for fungal ABC transporters, expression conferred on *S. cerevisiae* resistance to the known substrates aureobasidin A and R6G, and to ITC (Fig. 3B). The clarity of the AD/HsABCB1 R6G inhibitory zone, compared to the zone for AD/pABC3 cells, is partly due to efflux of (red) R6G from AD/HsABCB1 cells and retention of the dye by AD/pABC3 cells. The resistance phenotype conferred by HsAbcb1p was confirmed by liquid MIC assays. HsAbcb1p expression increased R6G resistance relative to that of AD/pABC3 16-fold (from 0.25 to 4 μg/ml), daunorubicin resistance 16-fold (from 2 to 32 μg/ml), and ITC resistance 40-fold (from 0.031 to 1.28 μg/ml). The faint Coomassie-stained band indicated in the HsAbcb1p lane of Fig. 4D was confirmed by matrix-assisted laser desorption ionization–time-of-flight mass spectrometry of tryptic fragments (42) to be HsAbcb1p (data not shown). The addition of a C-terminal GFP tag did not significantly affect the level of HsAbcb1p expression in the PM (Fig. 4D), but confocal microscopy indicated that most HsAbcb1p-GFP was localized inside the cell in membrane structures similar to those in cells overexpressing CneMdr1p (Fig. 7). Only a small proportion of the protein localized to the cell surface. It is not yet clear whether the apparent "mislocalization" was caused by the addition of the C-terminal GFP tag or whether it reflects the localization of the untagged protein.

**Identification of compounds that chemosensitize *S. cerevisiae* cells hyperexpressing membrane pumps to FLC.** The panel of strains overexpressing fungal drug pumps can be used in screens to identify and/or characterize broad-spectrum drug pump inhibitors that overcome the multidrug-resistant (MDR) phenotype of fungal pathogens. We therefore tested the abilities of eight known or suspected fungal ABC drug pump inhibitors to chemosensitize cells to FLC. The macrolide FK506 is widely used in cancer and organ transplant patients as an immunosuppressant. FK506 was originally discovered as an antifungal, and as an inhibitor of CaCdr1p (19) it reverses multidrug efflux in *C. albicans* (34, 53). The milbemycins are 16-membered ring macrolides belonging to families that are used as insecticides, acaricides, and anthelminthics (44, 60). Some milbemycins have also been identified as chemosensitizers of fungal multidrug efflux mediated by CaCdr1p (33). Enniatin is another circular molecule that has been found to inhibit antifungal drug efflux (25, 33). Oligomycin is used to distinguish fungal drug efflux pump ATPase activities from those of other PM ATPases, including the PM $H^+$ ATPase.

Chemosensitization to FLC of *S. cerevisiae* strains overex-